PeVatron studies with the Astri Mini-Array

A.Giuliani, S.Crestan, M.Rigoselli, A.Bonollo (IASF Milano), M.Cardillo (IAPS Roma)
A.D'Ai, F.Pintore (IASF Palermo), A.Tutone (OAR Roma)

for the ASTRI Project

ASTRI & LHAASO Workshop, 7-8 . 3 . 2023

Outline

Mini-Array

ASTRI and PeVatrons

- **Performances**
- **Strategy**

A few science cases

- **MGRO J1908+0621**
- **Cygnus Region**
- **SNR G106+2.7**
- **LHAASO J1956+2845**

ASTRI Performance

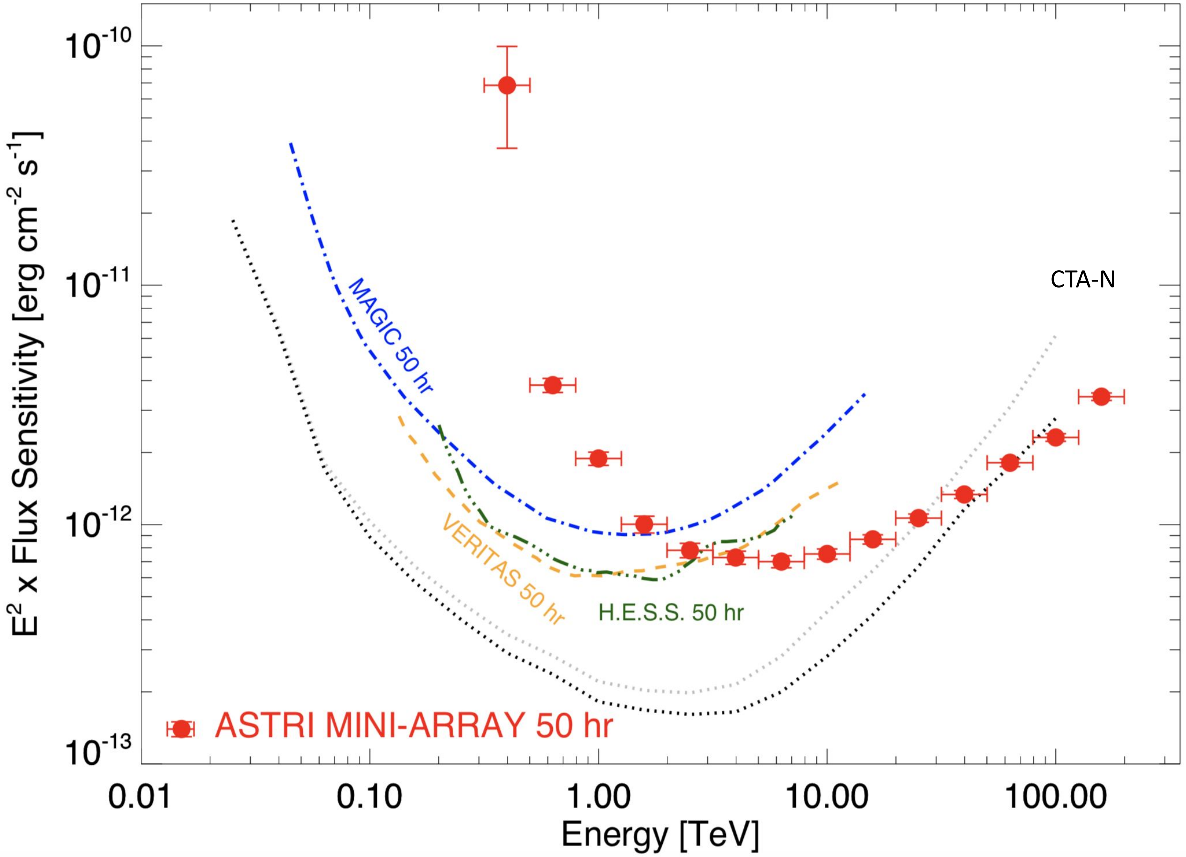

Expected performance

Sensitivity: better than that of current IACTs (E > a few TeV)

- Extend the spectra of already detected sources and/or measure cut-offs

ASTRI Performance

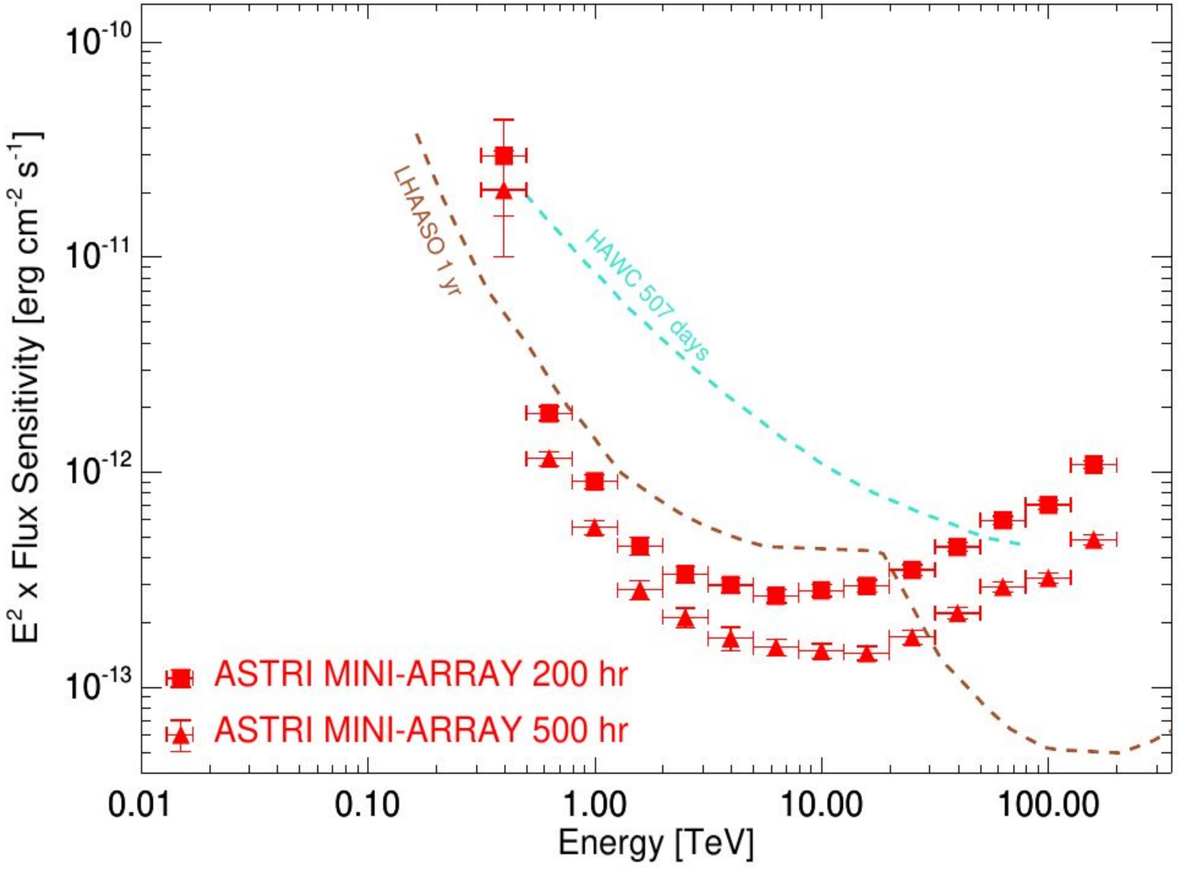

Expected performance

Sensitivity: better than that of current IACTs (E > a few TeV)

- Extend the spectra of already detected sources and/or measure cut-offs

ASTRI Performance

Mini-Array

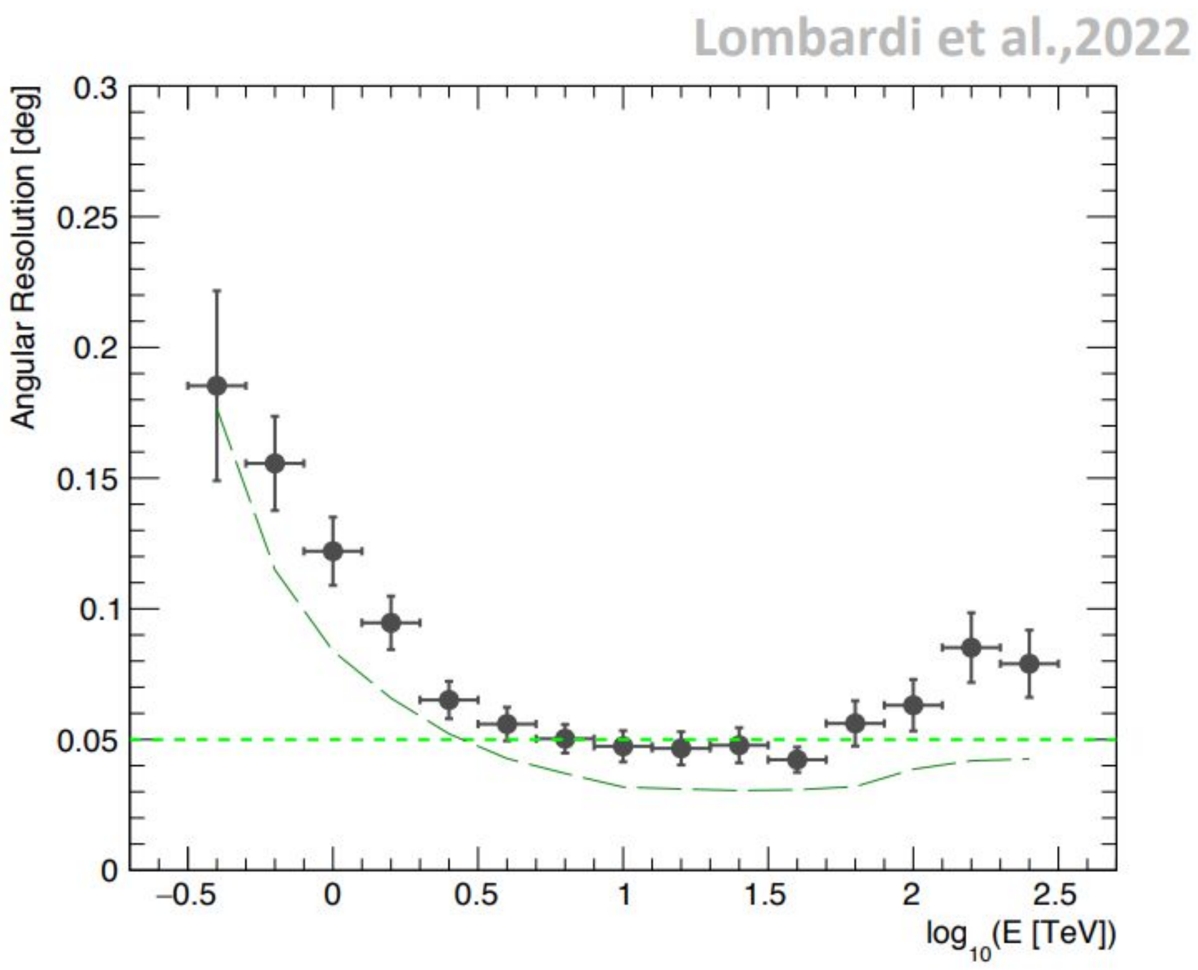

Expected performance

Sensitivity: better than that of current IACTs (E > a few TeV)

- Extend the spectra of already detected sources and/or measure cut-offs

Energy/Angular resolution: ~ 10% / ~ 3‘ (E > a few TeV)

- Characterize the morphology of extended sources at the highest VHE

ASTRI Performance

Mini-Array

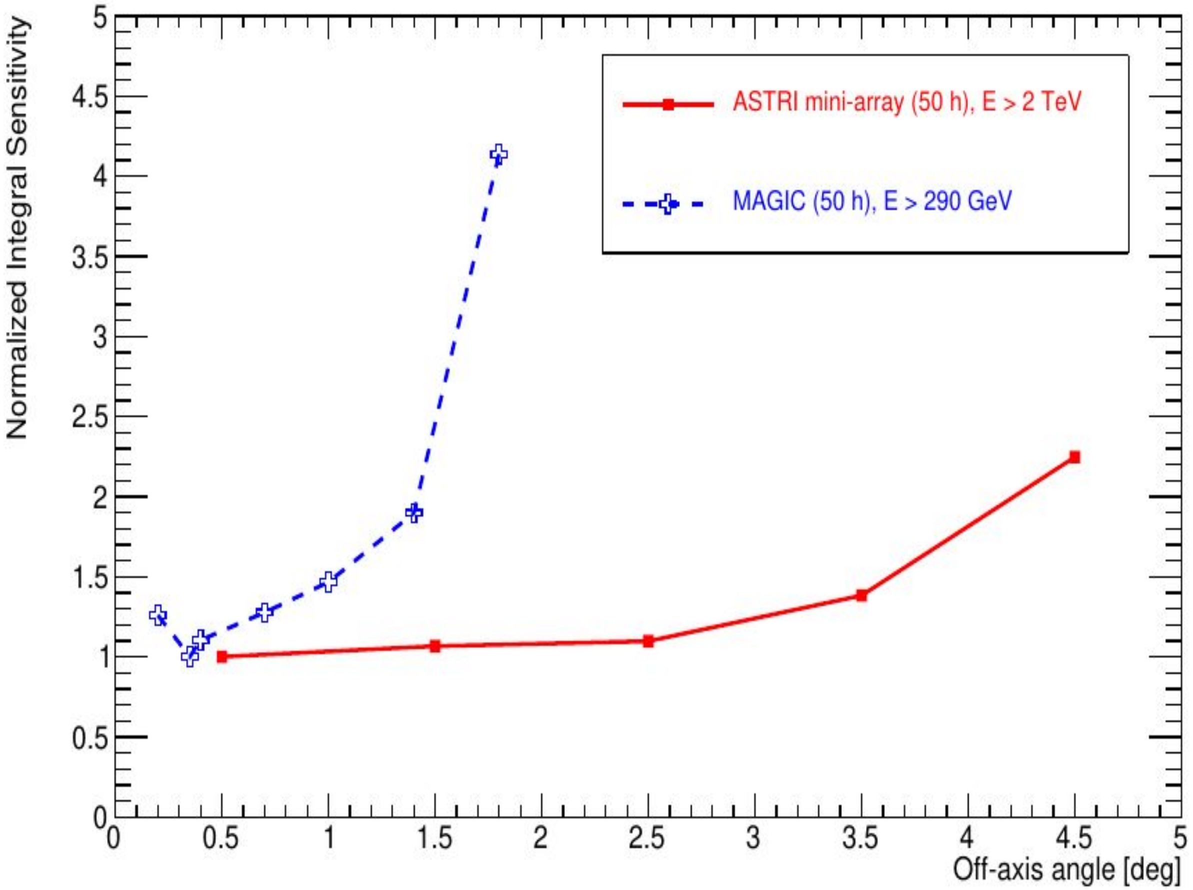

Expected performance

Sensitivity: better than that of current IACTs (E > a few TeV)

- Extend the spectra of already detected sources and/or measure cut-offs

Energy/Angular resolution: ~ 10% / ~ 3‘ (E > a few TeV)

- Characterize the morphology of extended sources at the highest VHE

Wide FoV (≥ 10°), with almost homogeneous off-axis acceptance

- Optimal for multi-target fields, surveys, and extended sources
- Enhanced chance for serendipity discoveries

Observing Plan

Strategy :

Focus on few sky fields in order to obtain long exposures

3 aces up the sleeve :

- Large FoV
  → Several sources in the FOV
- Observations with moonlight
  → Increases avail. time ~50-80%
- Large Z.A.
  → Increase Aeff @ high energies

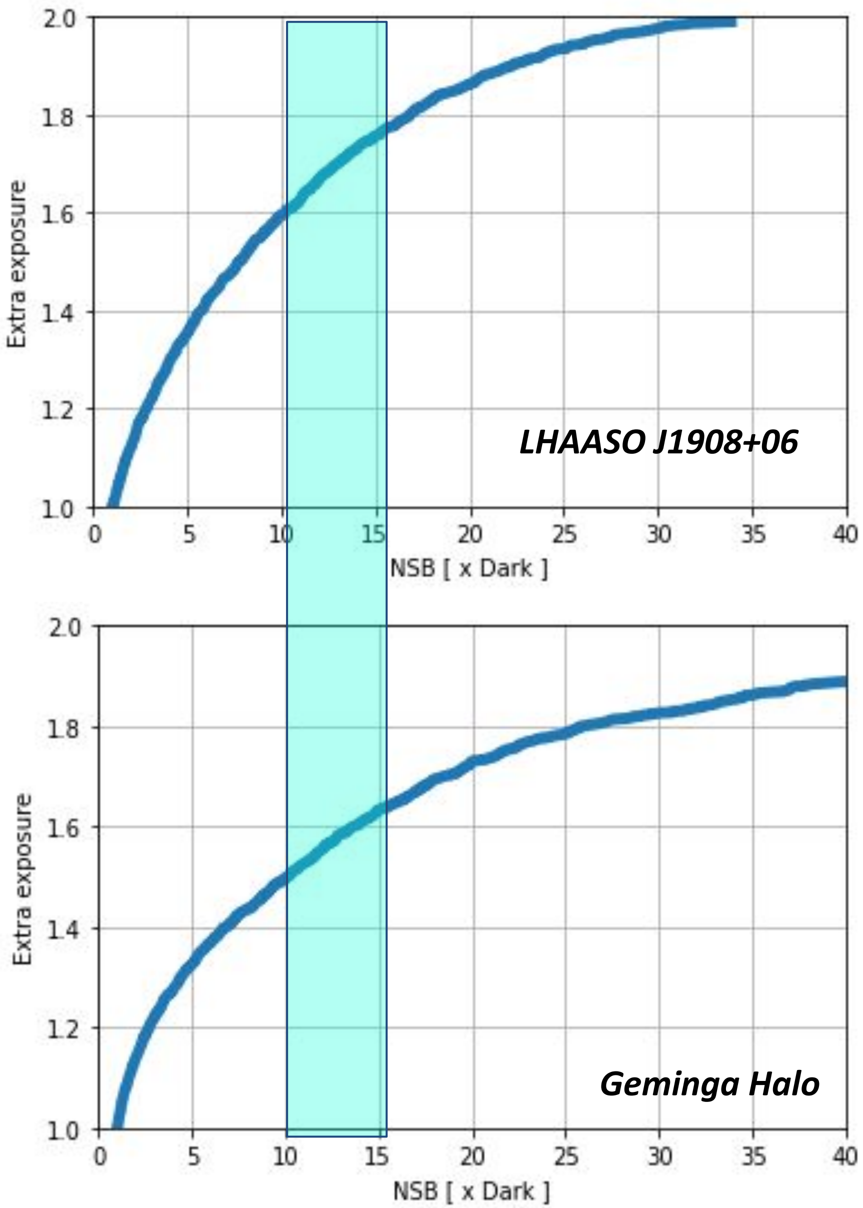

Outline

ASTRI Mini-Array

ASTRI and PeVatrons

- Performances
- Strategy

A few science cases

- Cygnus Region
- LHAASO J1908+0621
- SNR G106+2.7
- LHAASO J1956+2845

LHAASO Sources : Cygnus Region

Source name	RA (°)	dec. (°)	Significance above 100 TeV (×σ)	E_{max} (PeV)	Flux at 100 TeV (CU)
LHAASO J0534+2202	83.55	22.05	17.8	0.88 ± 0.11	1.00(0.14)
LHAASO J1825-1326	276.45	−13.45	16.4	0.42 ± 0.16	3.57(0.52)
LHAASO J1839-0545	279.95	−5.75	7.7	0.21 ± 0.05	0.70(0.18)
LHAASO J1843-0338	280.75	−3.65	8.5	$0.26 -0.10^{+0.16}$	0.73(0.17)
LHAASO J1849-0003	282.35	−0.05	10.4	0.35 ± 0.07	0.74(0.15)
LHAASO J1908+0621	287.05	6.35	17.2	0.44 ± 0.05	1.36(0.18)
LHAASO J1929+1745	292.25	17.75	7.4	$0.71 -0.07^{+0.16}$	0.38(0.09)
LHAASO J1956+2845	299.05	28.75	7.4	0.42 ± 0.03	0.41(0.09)
LHAASO J2018+3651	304.75	36.85	10.4	0.27 ± 0.02	0.50(0.10)
LHAASO J2032+4102	308.05	41.05	10.5	1.42 ± 0.13	0.54(0.10)
LHAASO J2108+5157	317.15	51.95	8.3	0.43 ± 0.05	0.38(0.09)
LHAASO J2226+6057	336.75	60.95	13.6	0.57 ± 0.19	1.05(0.16)

Celestial coordinates (RA, dec.); statistical significance of detection above 100 TeV (calculated using a point-like template for the Crab Nebula and LHAASO J2108+5157 and 0.3° extension templates for the other sources); the corresponding differential photon fluxes at 100 TeV; and detected highest photon energies. Errors are estimated as the boundary values of the area that contains ±34.14% of events with respect to the most probable value of the event distribution. In most cases, the distribution is a Gaussian and the error is 1σ.

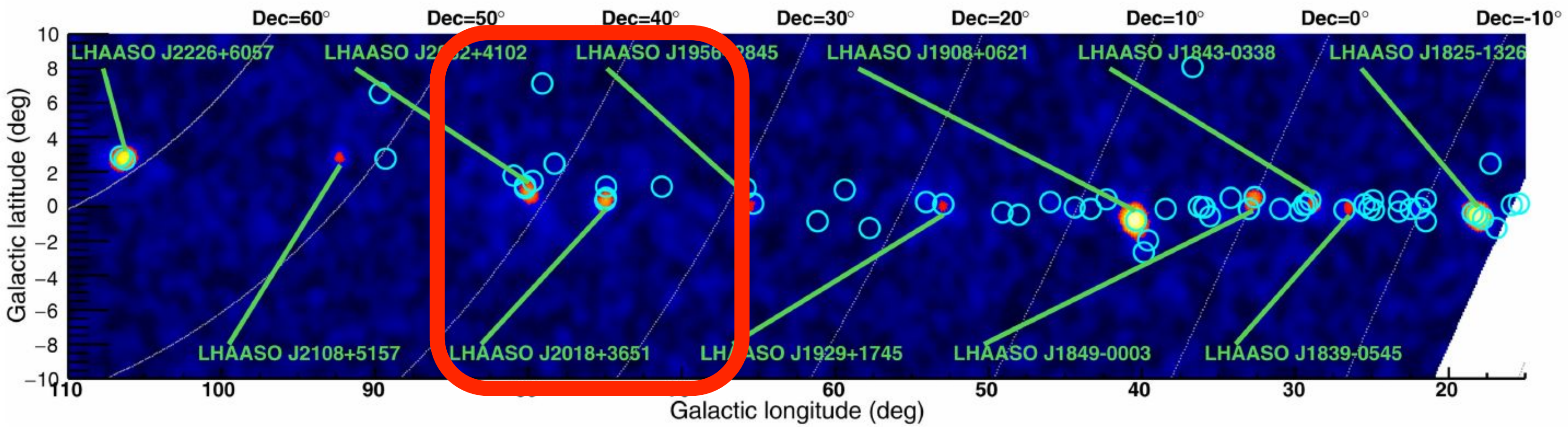

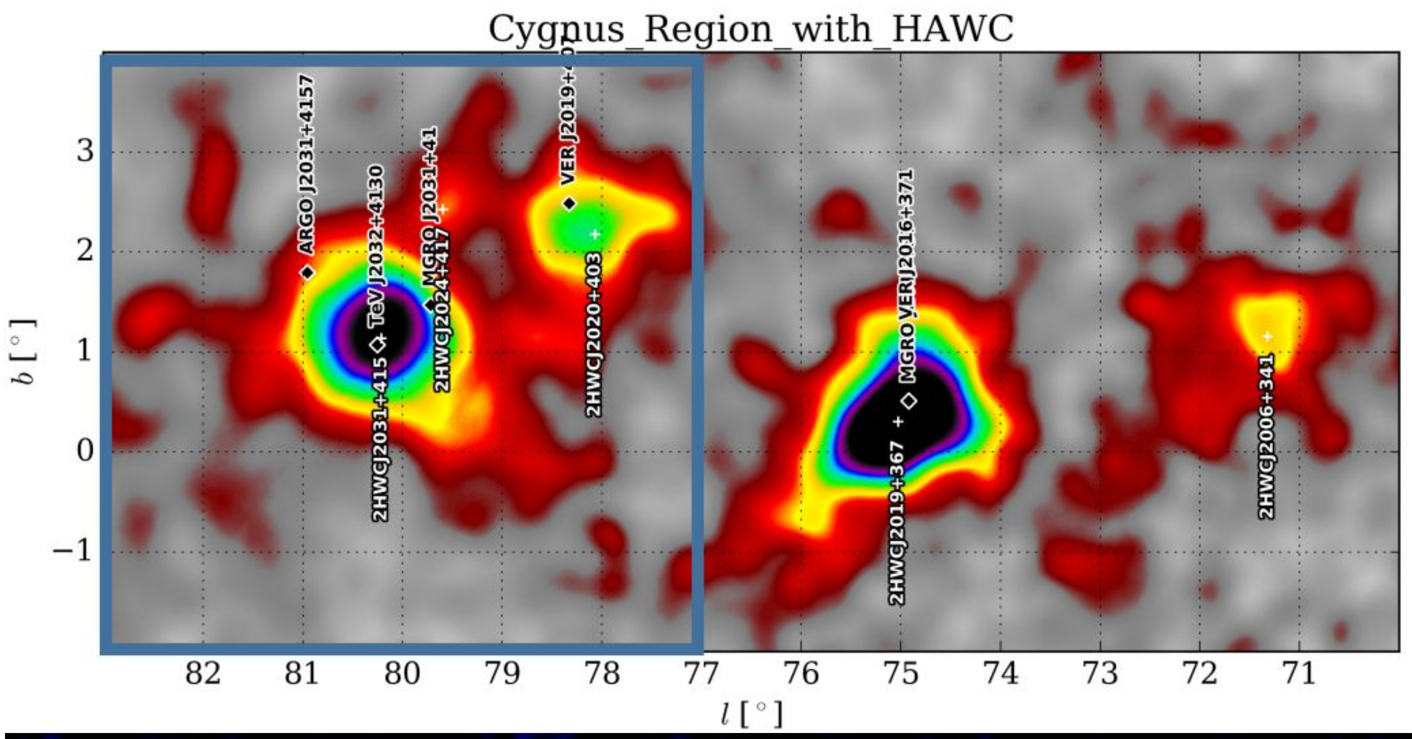

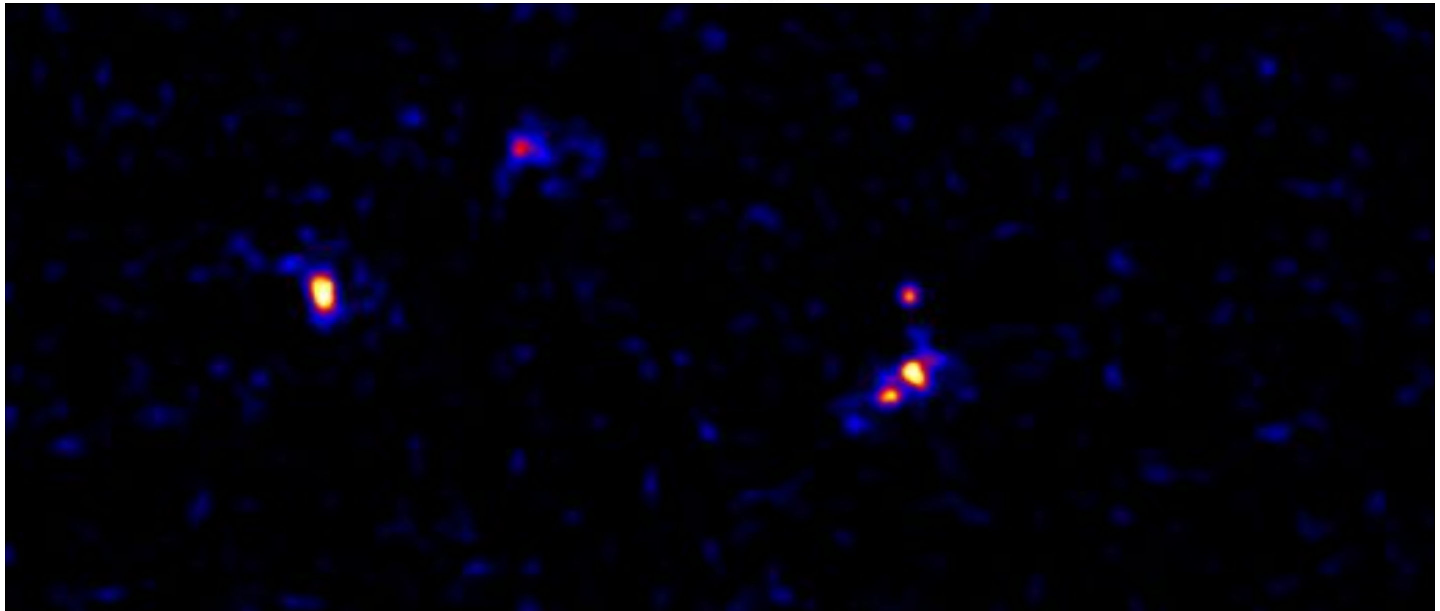

Cygnus Region

seen by HAWC
(E > 8 TeV)

seen by Veritas
(E > 200 GeV)

The data challenge of the Cygnus region

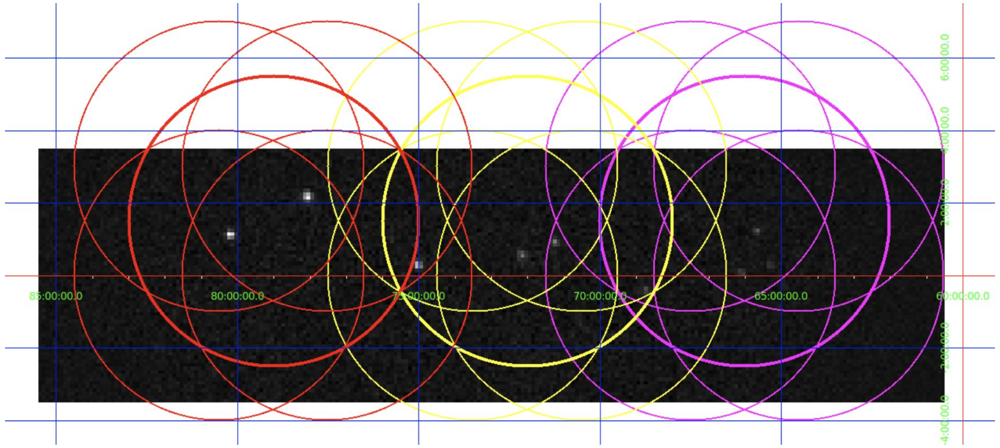

We simulated a survey of the Cygnus region, adopting 15 pointing positions along the Galactic longitude in the [60-85 deg] range.

All the known sources (eg from 3rd HAWC catalogue + LHAASO) and the Galactic diffuse component (from Gaggiero et al.) were simulated.

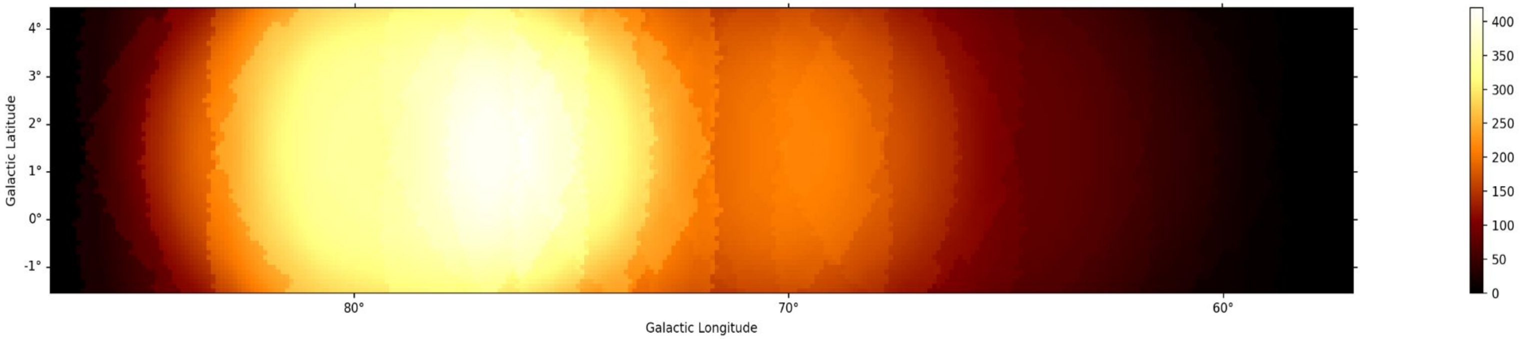

Background map of the region,
brightness indicates regions of higher ***exposure***

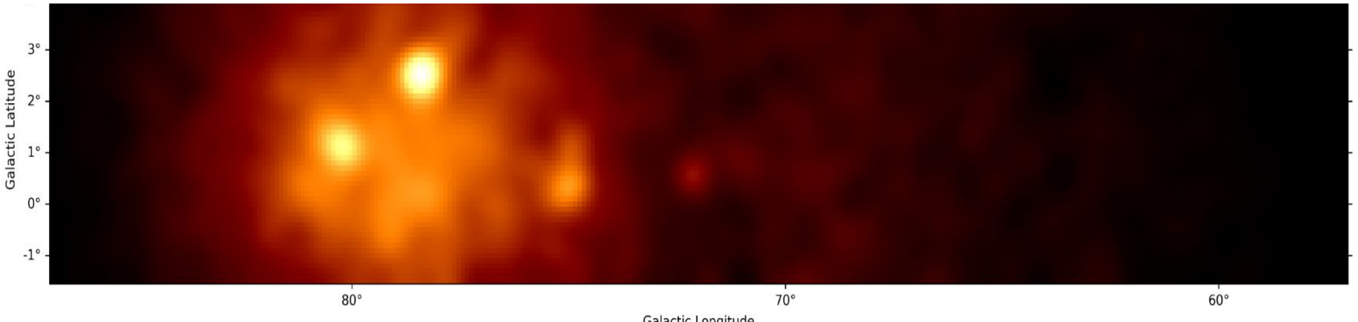

Excess map of the region,
brighter points indicate ***source or diffuse emission***

LHAASO J2018+3651 - Overview

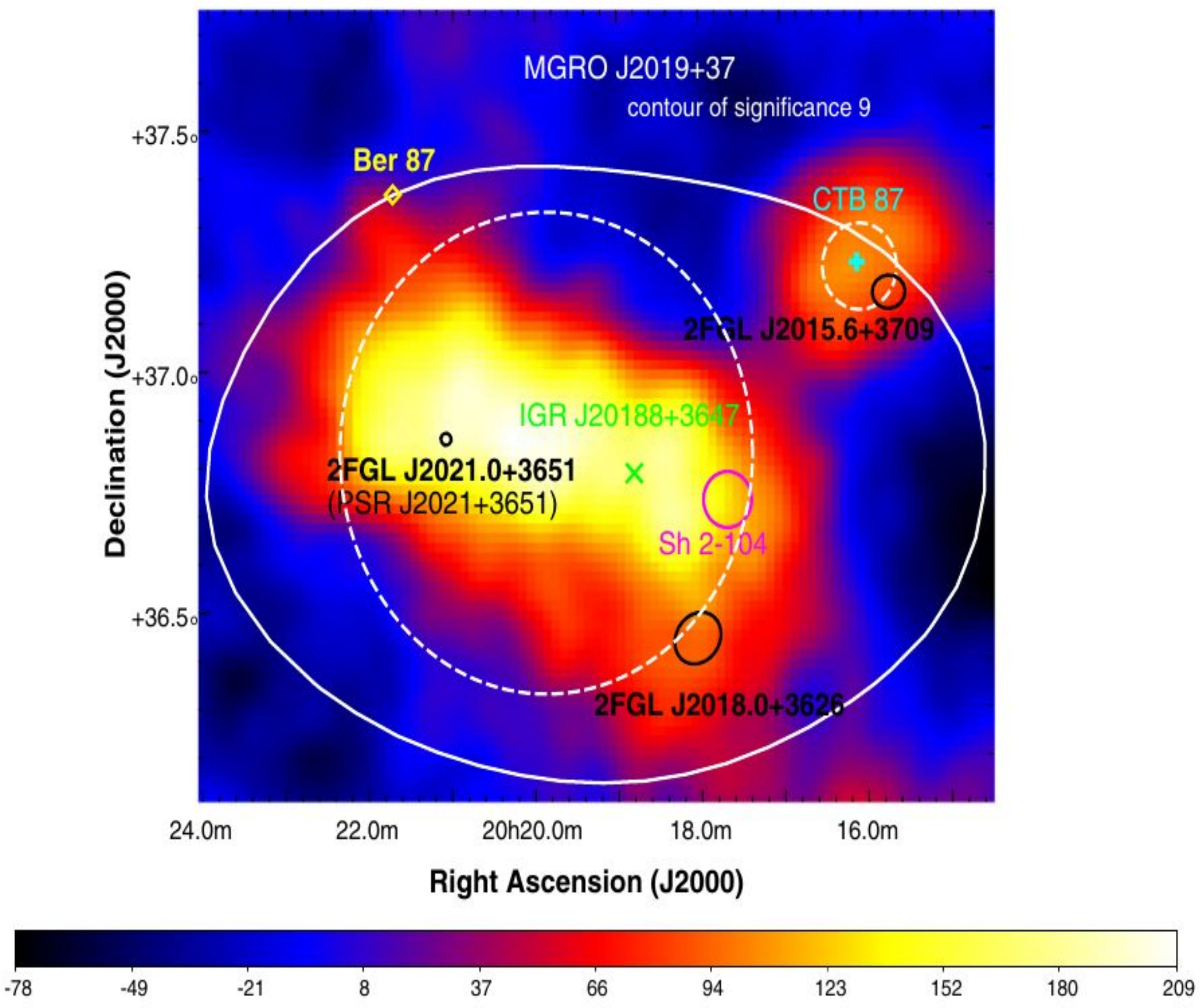

From : The Astrophysical Journal, 788:78 (10pp), 2014

VERITAS Cygnus Region Survey - Abeysekara et al. 2018

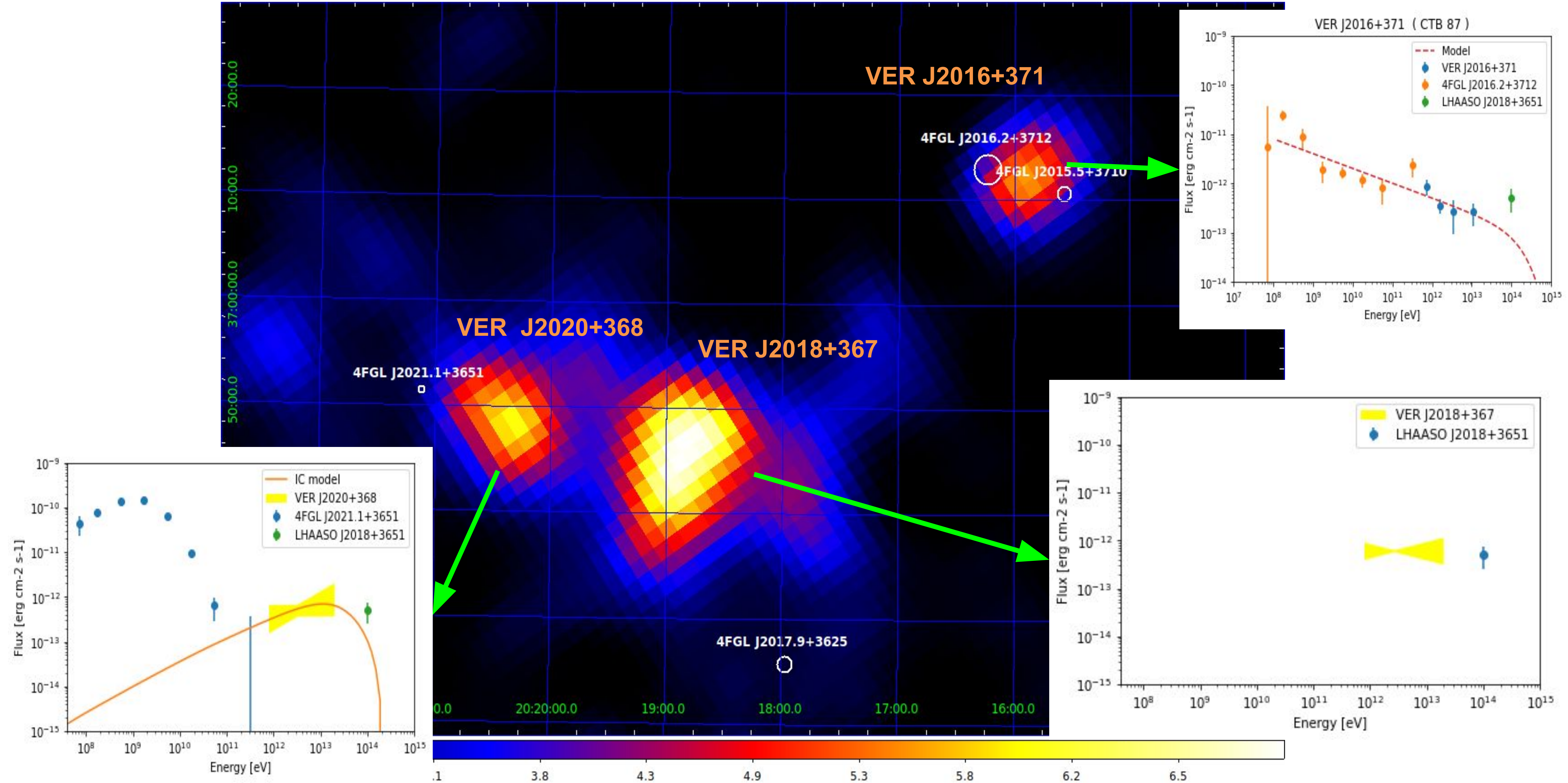

LHAASO J2018+3651

ASTRI M.A. observations
Exposure : 200 hrs

Spectral Parameters			
Name	N_0	Γ	λ
Source A	$(4.6\pm0.4)\times10^{-15}$	1.8 ± 0.04	0.01 ± 0.004
Source B	$(3.9\pm0.6)\times10^{-15}$	1.8 ± 0.06	0.004 ± 0.002
Source C	$(9.0\pm0.3)\times10^{-16}$	2.5 ± 0.09	-
Spatial Parameters			
Name	l	b	σ
Source A	75.11 ± 0.02	0.2 ± 0.008	0.056 ± 0.005
Source B	74.89 ± 0.02	0.44 ± 0.009	0.04 ± 0.003
Source C	$74.95\ \pm0.01$	1.18 ± 0.009	0.02 ± 0.008

Counts Map

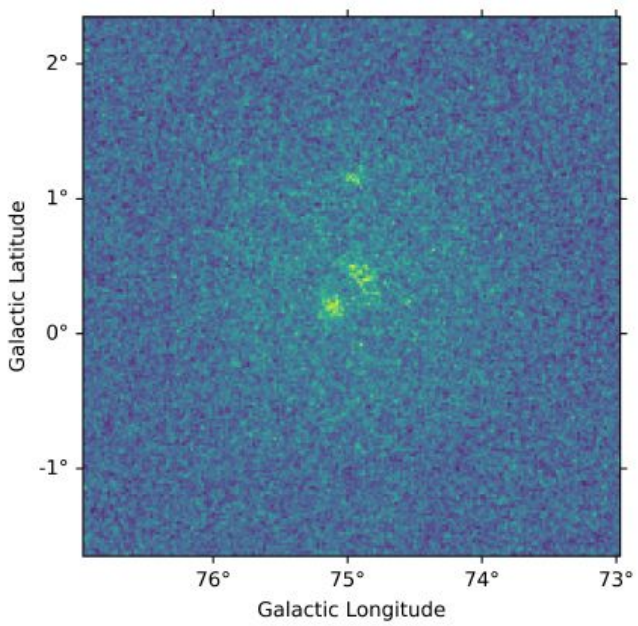

Significance

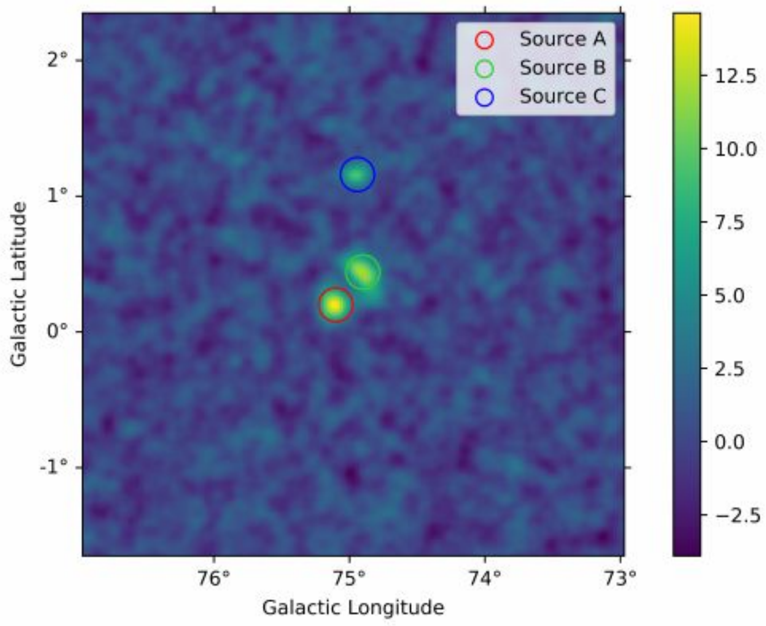

Source	l	b	TS
	deg	deg	
Source A	305.09	36.80	214
Source B	304.70	36.77	147
Source C	303.99	37.21	90

LHAASO J2018+3651

ASTRI M.A. observations
Exposure : 200 hrs

Spectral Parameters			
Name	N_0	Γ	λ
Source A	$(4.6\pm0.4)\times10^{-15}$	1.8 ± 0.04	0.01 ± 0.004
Source B	$(3.9\pm0.6)\times10^{-15}$	1.8 ± 0.06	0.004 ± 0.002
Source C	$(9.0\pm0.3)\times10^{-16}$	2.5 ± 0.09	-
Spatial Parameters			
Name	l	b	σ
Source A	75.11 ± 0.02	0.2 ± 0.008	0.056 ± 0.005
Source B	74.89 ± 0.02	0.44 ± 0.009	0.04 ± 0.003
Source C	$74.95\ \pm0.01$	1.18 ± 0.009	0.02 ± 0.008

Counts Map

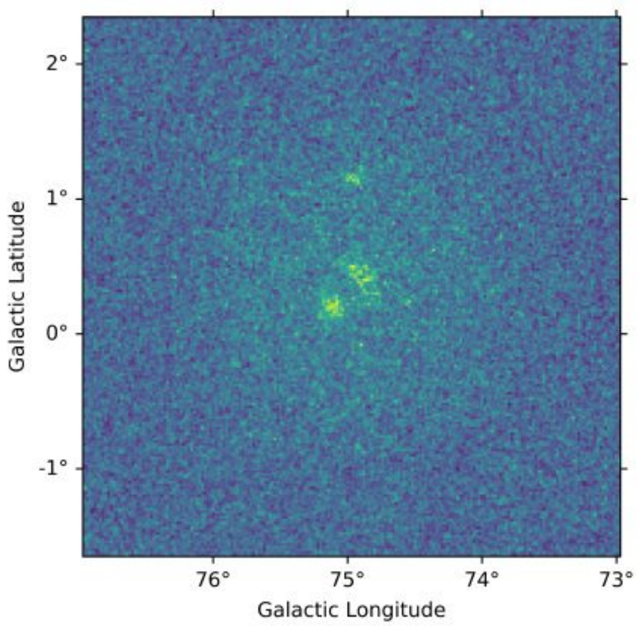

Significance

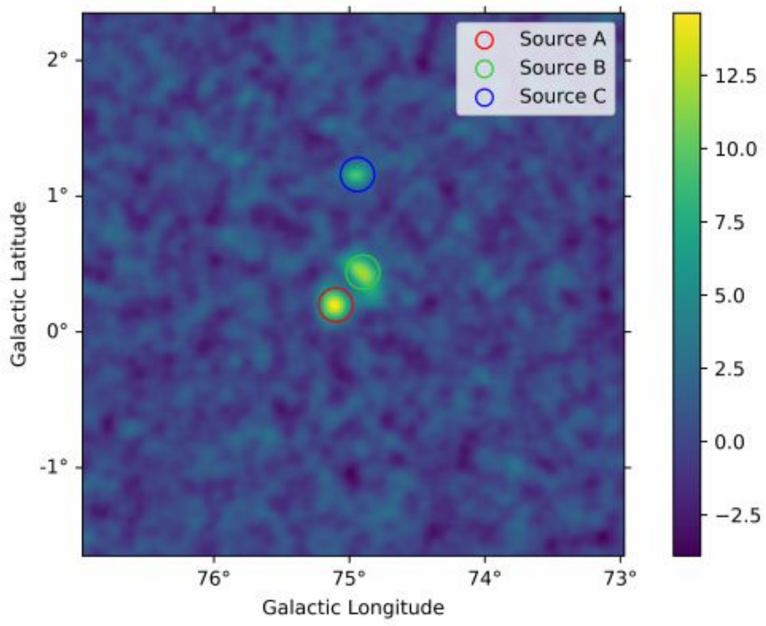

Residuals

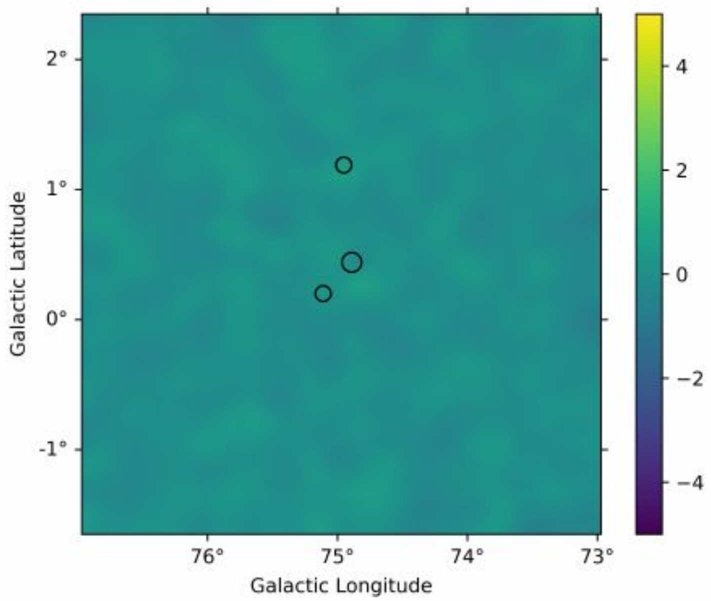

Outline

ASTRI and PeVatrons

- **Performances**
- **Strategy**

A few science cases

- **Cygnus Region**
- **LHAASO J1908+0621**
- **SNR G106+2.7**
- **LHAASO J1956+2845**

LHAASO Sources

Source name	RA (°)	dec. (°)	Significance above 100 TeV (×σ)	E_{max} (PeV)	Flux at 100 TeV (CU)
LHAASO J0534+2202	83.55	22.05	17.8	0.88 ± 0.11	1.00(0.14)
LHAASO J1825-1326	276.45	−13.45	16.4	0.42 ± 0.16	3.57(0.52)
LHAASO J1839-0545	279.95	−5.75	7.7	0.21 ± 0.05	0.70(0.18)
LHAASO J1843-0338	280.75	−3.65	8.5	$0.26 -0.10^{+0.16}$	0.73(0.17)
LHAASO J1849-0003	282.35	−0.05	10.4	0.35 ± 0.07	0.74(0.15)
LHAASO J1908+0621	287.05	6.35	17.2	0.44 ± 0.05	1.36(0.18)
LHAASO J1929+1745	292.25	17.75	7.4	$0.71 -0.07^{+0.16}$	0.38(0.09)
LHAASO J1956+2845	299.05	28.75	7.4	0.42 ± 0.03	0.41(0.09)
LHAASO J2018+3651	304.75	36.85	10.4	0.27 ± 0.02	0.50(0.10)
LHAASO J2032+4102	308.05	41.05	10.5	1.42 ± 0.13	0.54(0.10)
LHAASO J2108+5157	317.15	51.95	8.3	0.43 ± 0.05	0.38(0.09)
LHAASO J2226+6057	336.75	60.95	13.6	0.57 ± 0.19	1.05(0.16)

Celestial coordinates (RA, dec.); statistical significance of detection above 100 TeV (calculated using a point-like template for the Crab Nebula and LHAASO J2108+5157 and 0.3° extension templates for the other sources); the corresponding differential photon fluxes at 100 TeV; and detected highest photon energies. Errors are estimated as the boundary values of the area that contains ±34.14% of events with respect to the most probable value of the event distribution. In most cases, the distribution is a Gaussian and the error is 1σ.

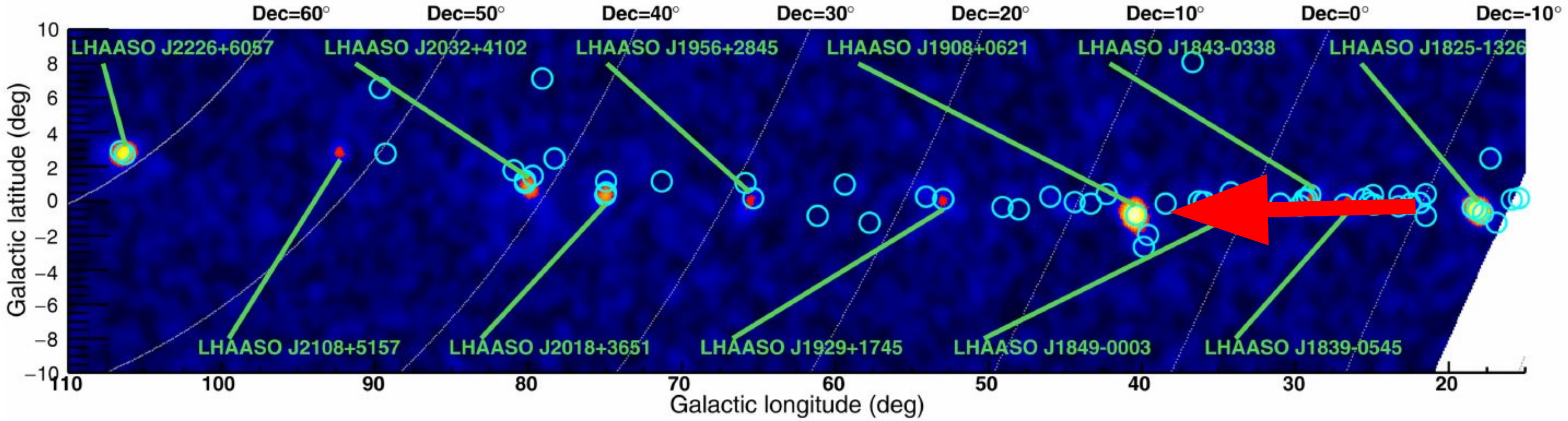

LHAASO Sources

LHAASO J1908+0621

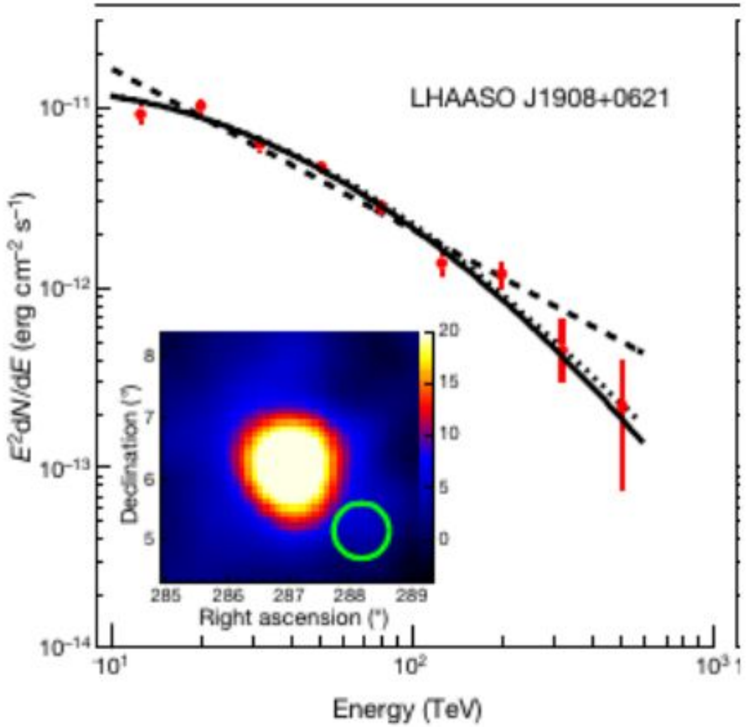

source	Number of on-source events	number of background events	exposure (hr)
LHAASO J0534+2202	67	5.5	2236.4
LHAASO J1825-1326	61	3.2	1149.3
LHAASO J1839-0545	26	4.2	1614.5
LHAASO J1843-0338	30	4.3	1715.4
LHAASO J1849-0003	36	4.8	1865.3
LHAASO J1908+0621	74	5.1	2058.0
LHAASO J1929+1745	29	5.8	2282.6
LHAASO J1956+2845	34	6.1	2461.5
LHAASO J2018+3651	42	6.3	2610.7
LHAASO J2032+4102	45	6.7	2648.2
LHAASO J2108+5157	30	6.4	2525.8
LHAASO J2226+6057	60	6.2	2401.3

Ultrahigh-energy photons up to 1.4 petaelectronvolts from 12 Î³-ray Galactic sources (LAHAASO coll.Â Nature, 2021)

LHAASO J1908+0621

Source counterparts

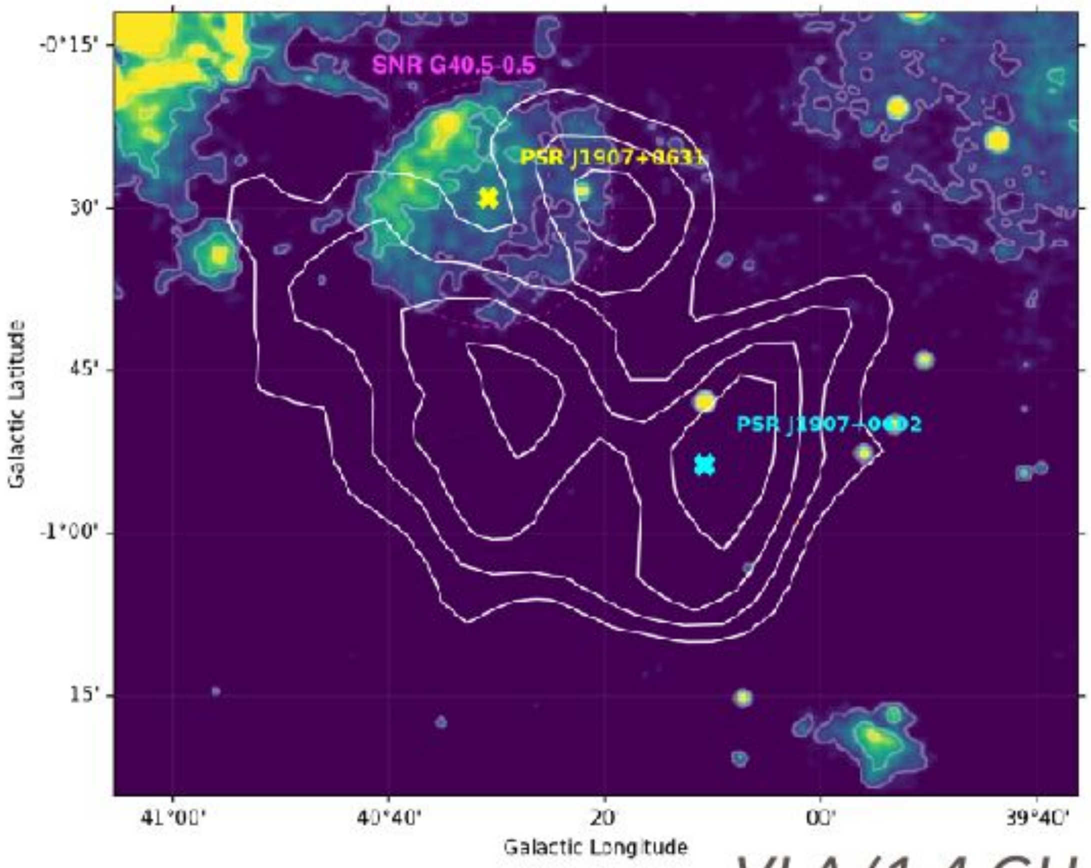

VLA (1.4 GHz)

VERITAS (E>200 GeV)

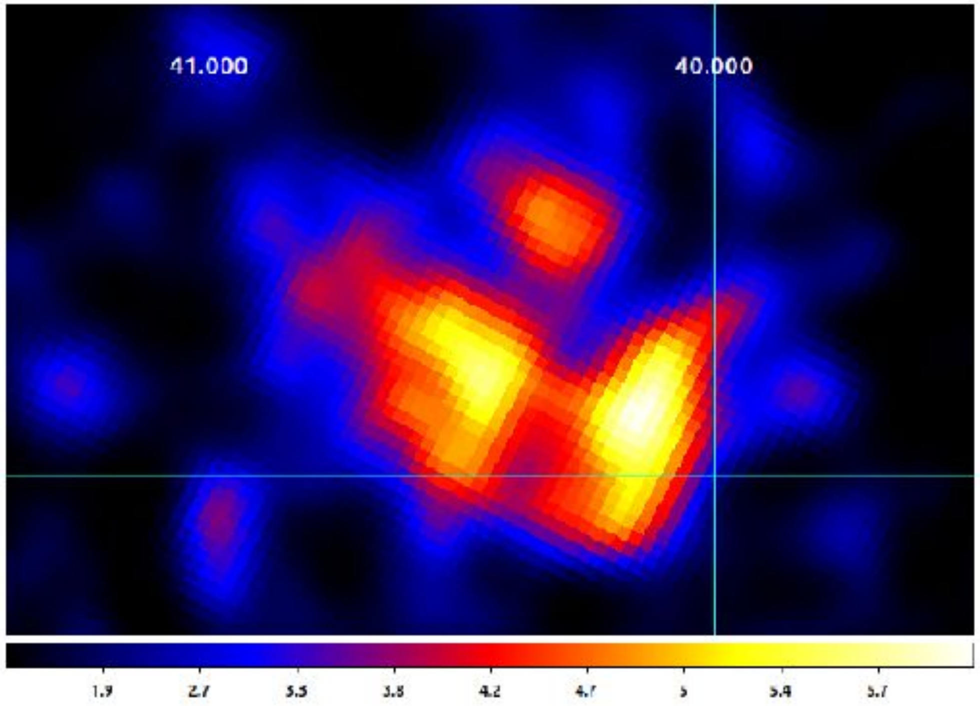

LHAASO J1908+0621

CO emission

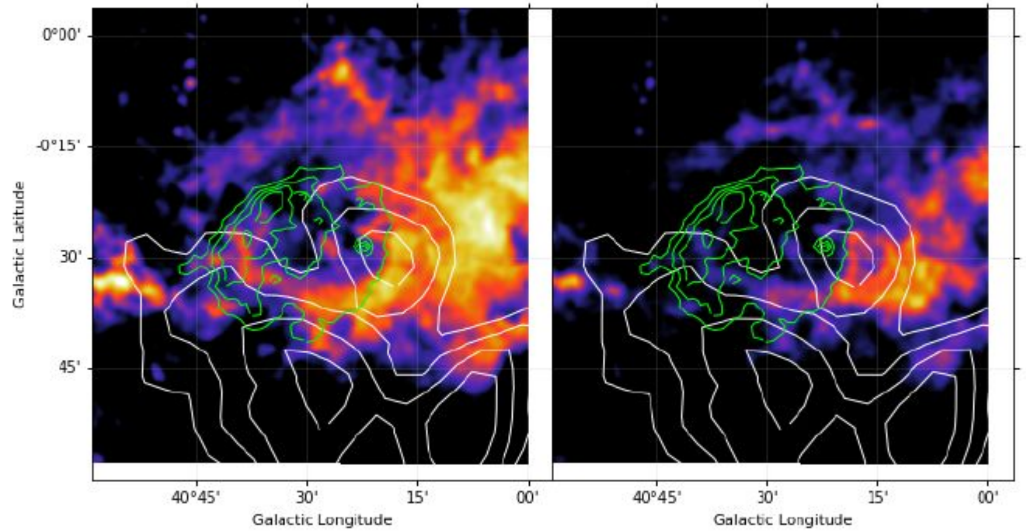

Maps of the 12CO (left) and 13CO (right) emission in the region integrated between 58 - 62 km s-1

Crestan et al. MNRAS, 2021

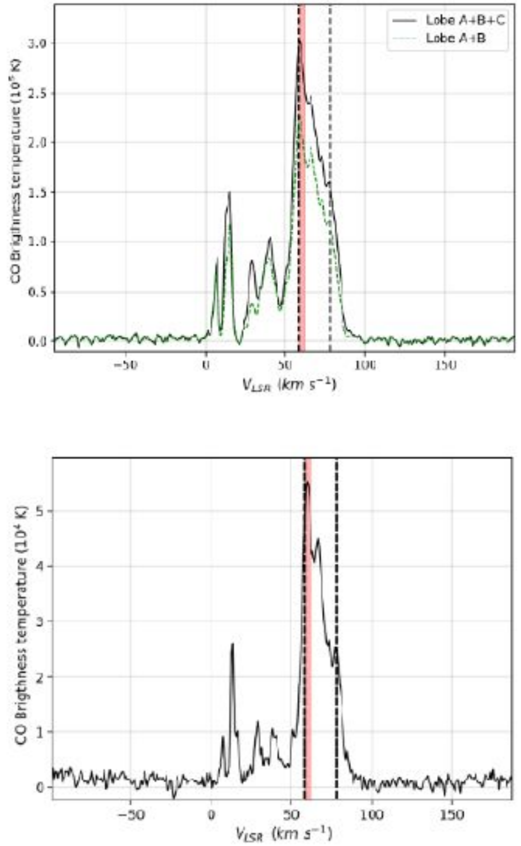

Figure 2. The ^{12}CO (top) and ^{13}CO (bottom) summed spectra in the region of MGRO J1908+06. The velocity interval between the two dashed lines (58–78 km s^{-1}) represents the bulk of the emission, while the red zone marks the velocity range between 58 and 62 km s^{-1} (shown in Fig. 3) that is the velocity range considered for the molecular cloud analysis (section 3.1).

LHAASO J1908+0621

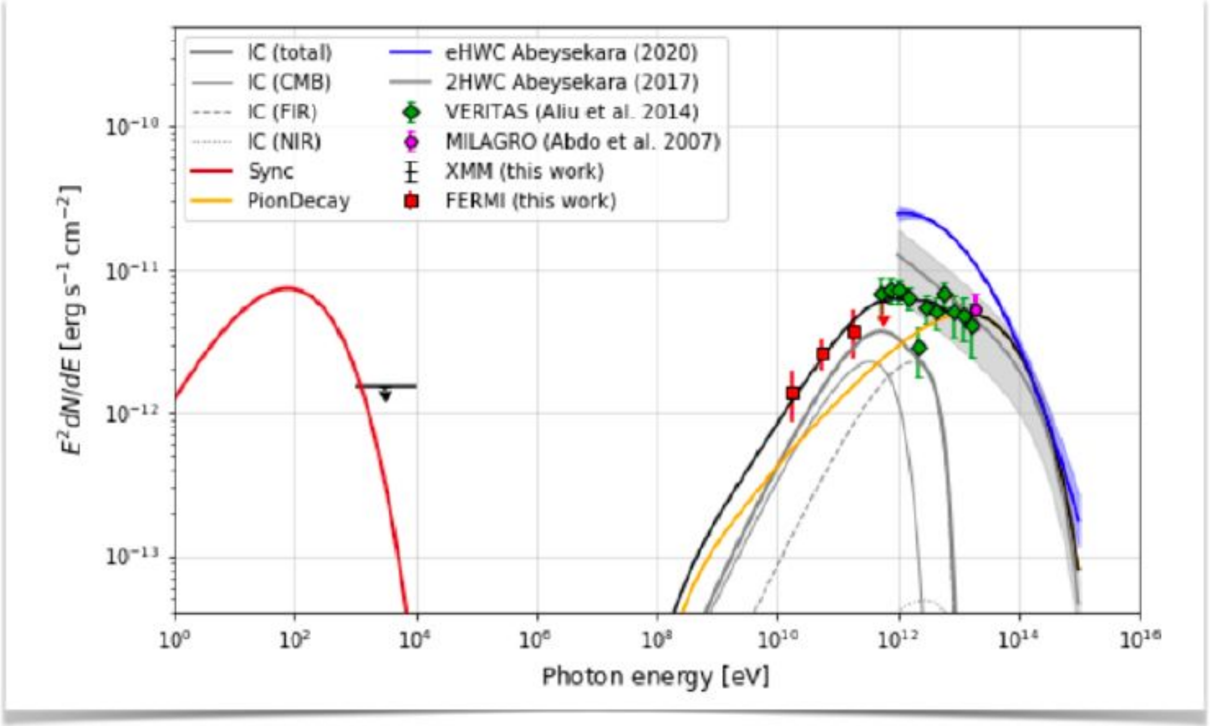

Model	Component	d (kpc)	Γ_1	Γ_2	W (erg)	E_0 (TeV)	E_b (TeV)	E_c (PeV)
1-zone	Leptonic	3	1.0 ± 0.4	2.6 ± 0.1	2×10^{47}	10	2.7 ± 0.7	7.1 ± 6.0
1-zone	Hadronic	3	1.0 ± 0.1	2.1 ± 0.1	7×10^{47}	30	2.8 ± 0.8	3.0 ± 0.9
1-zone	Hadronic	9	1.1 ± 0.2	2.1 ± 0.1	2×10^{49}	30	3.4 ± 1.2	1.9 ± 0.5
2-component	Leptonic	3	1.2	1.2	9×10^{46}	10	0.2	0.011
	Hadronic	3	1.6	2.0	4×10^{47}	30	200	>1
	Hadronic	9	1.6	2.0	1×10^{49}	30	200	>1

Crestan et al. MNRAS, 2021

Follow up of LHAASO sources : the case of J1908+0621

ASTRI Mini-Array **200 hr simulation (up to E~200 TeV)** of 2HWC J1908+063

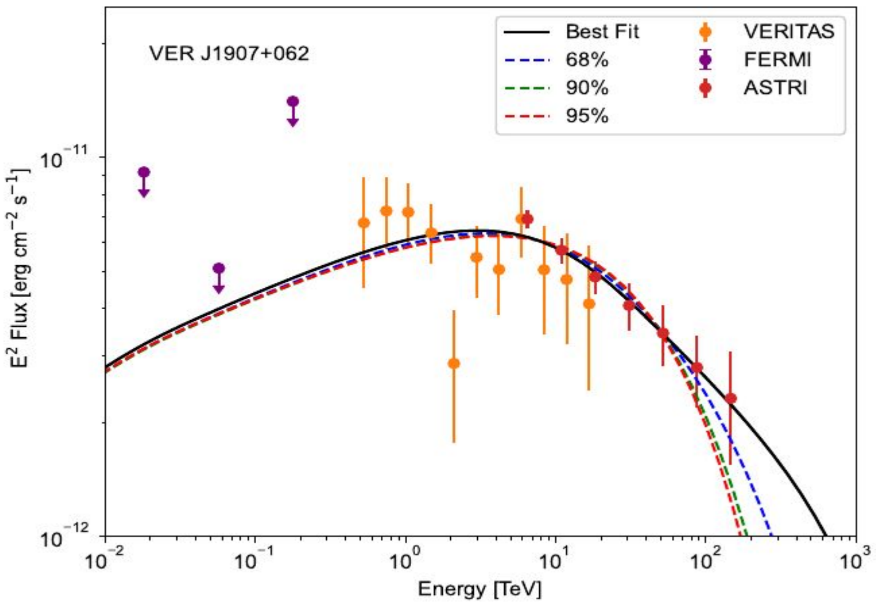

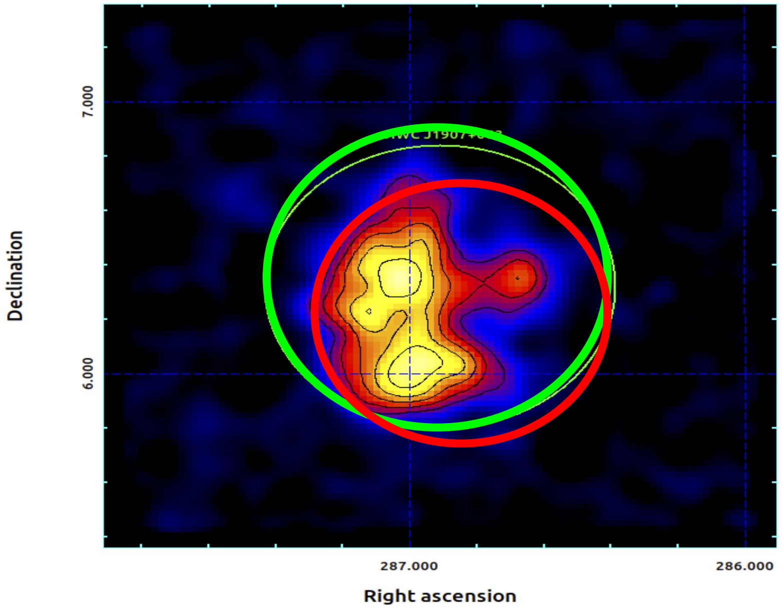

The light green circle marks the ~ 0.52° HAWC error-box

Follow up of LHAASO sources : the case of J1908+0621

ASTRI Mini-Array **200 hr simulation (up to E~200 TeV)**
of [2HWC J1908+063]()

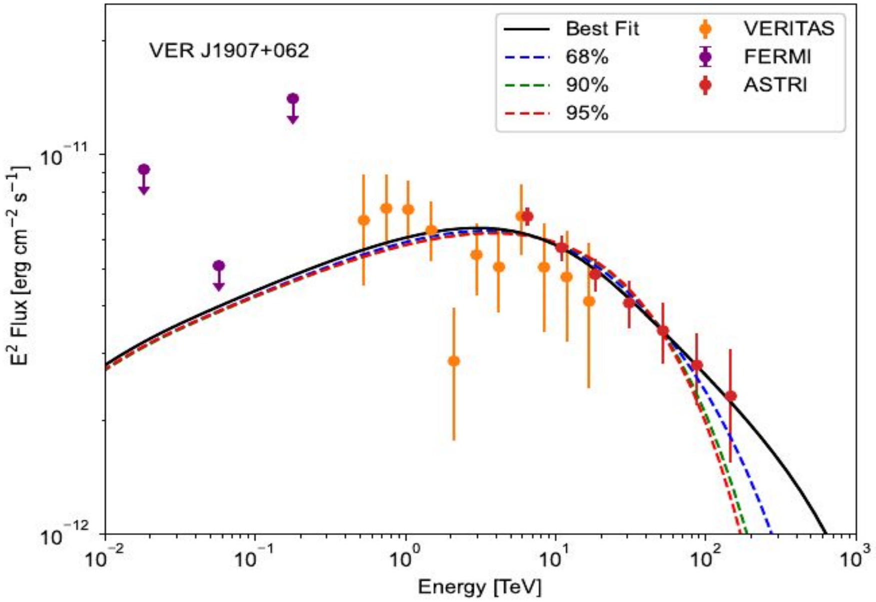

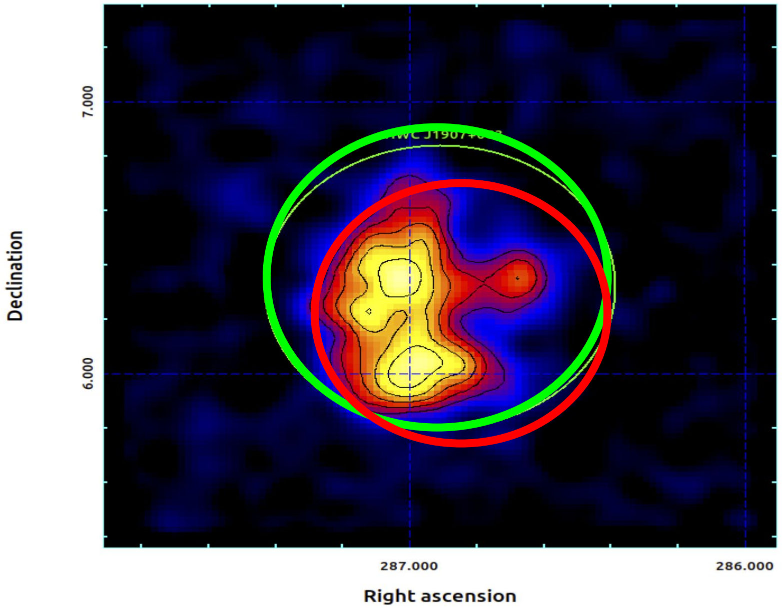

The light green circle marks the ~ 0.52° HAWC error-box

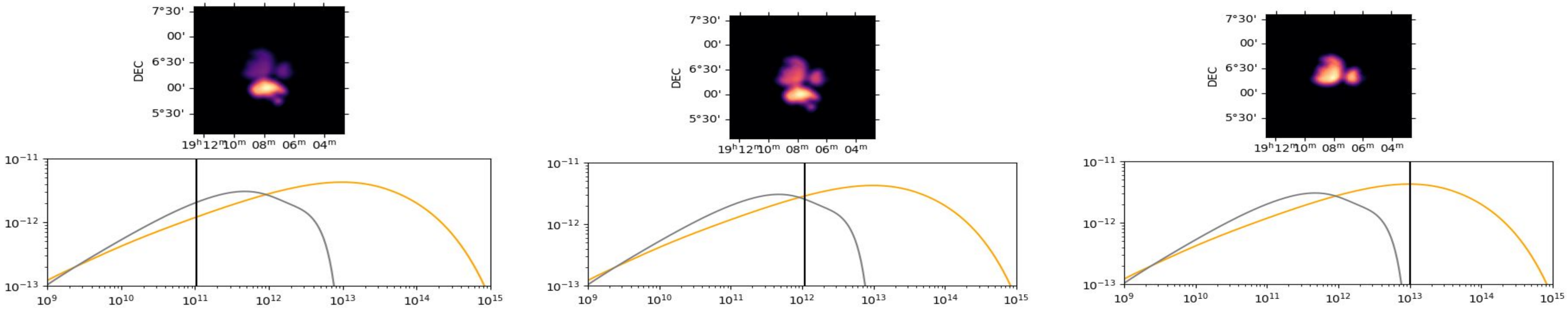

An Energy-dependent morphology (2 zone model)
can be **resolved by the ASTRI observations**

Follow up of LHAASO sources : the case of J1908+0621

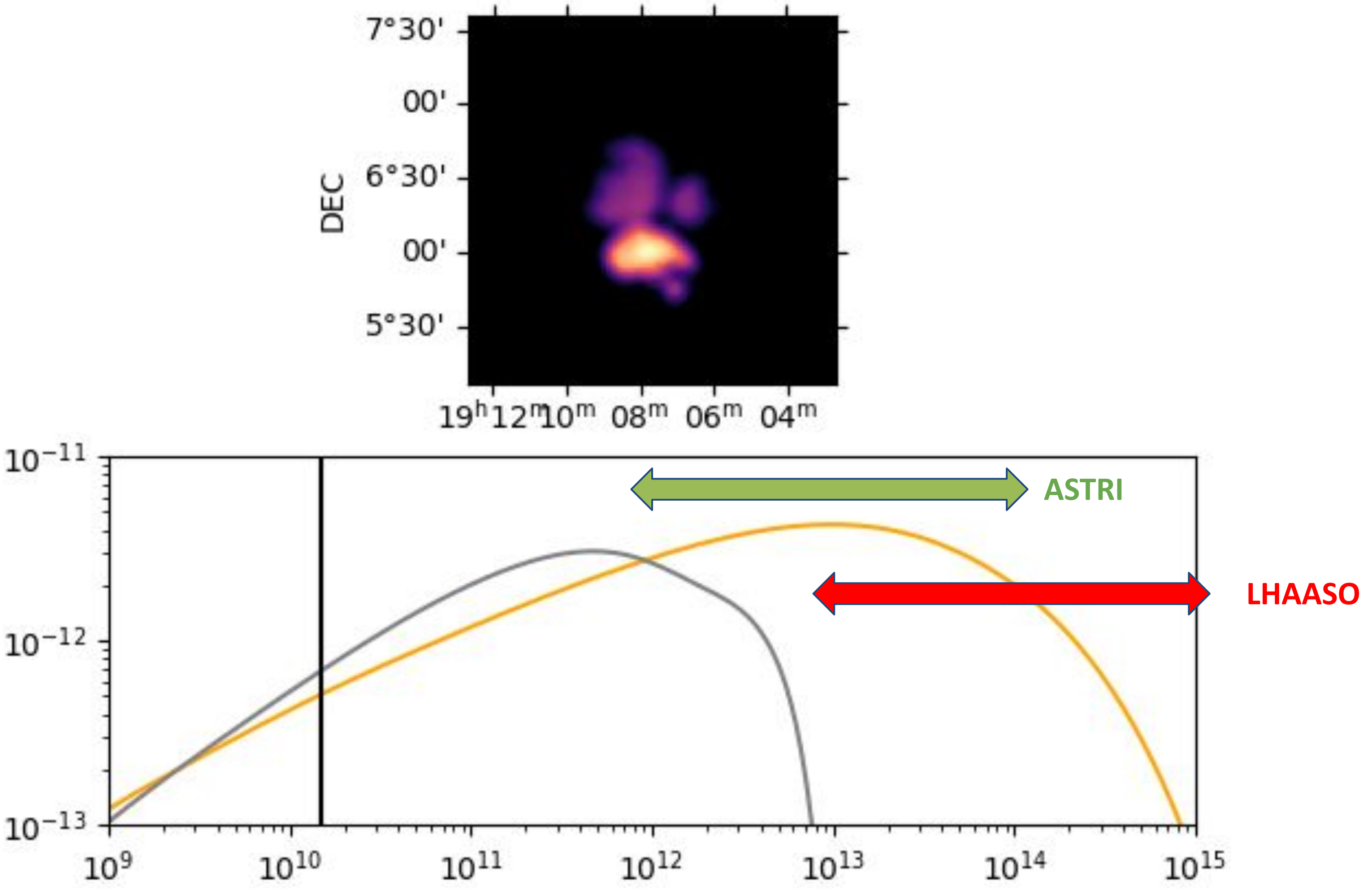

Outline

ASTRI and PeVatrons

- Performances
- Strategy

A few science cases

- Cygnus Region
- LHAASO J1908+0621
- SNR G106+2.7
- LHAASO J1956+2845

SNR G106.3+2.7

- TeV emission extended (energy dependent)
- 0.4° from PSR J2229+6114
- Detected by FERMI, MAGIC, VERITAS, Milagro, HAWC, Tibet AS-γ, LHAASO
- Overlaps with region of high CO density

MAGIC results

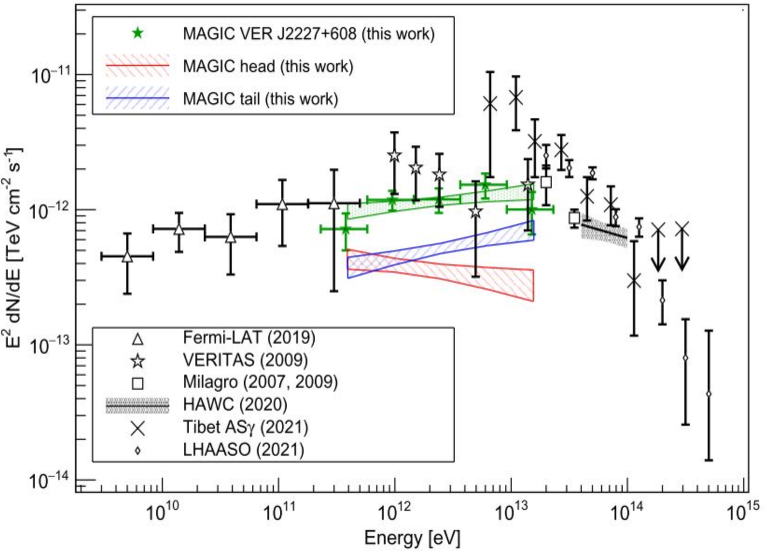

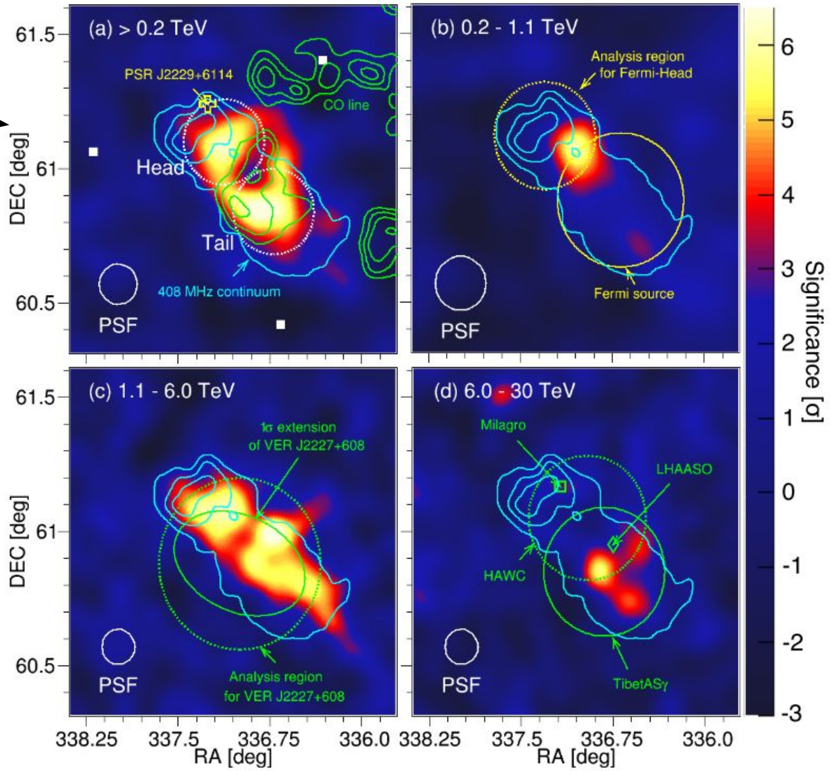

What we did in core science paper:

- Morphology and spectrum from VERITAS
- Ellipse (0.27° - 0.18°)
- 5% Crab Flux (>1 TeV)
- Power-law (Γ = 2.29)

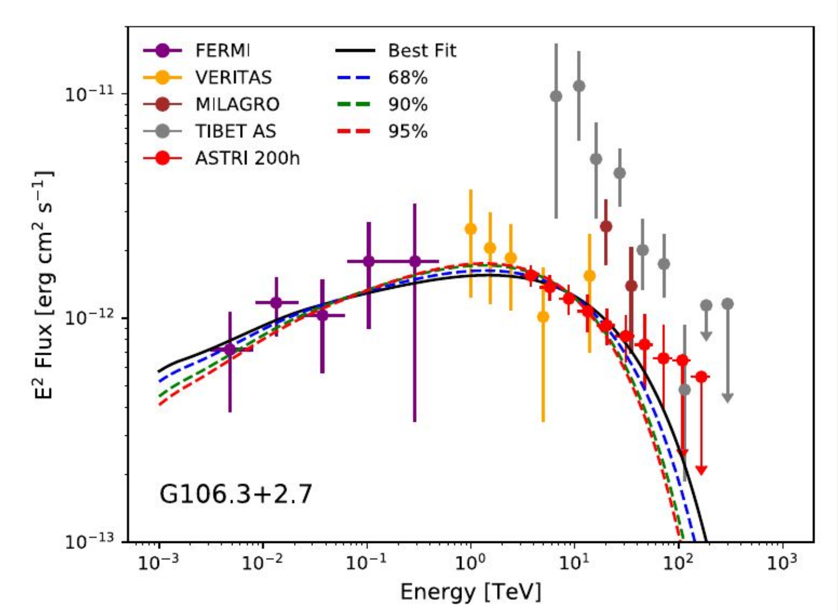

Outline

ASTRI and PeVatrons

- Performances
- Strategy

A few science cases

- Cygnus Region
- LHAASO J1908+0621
- SNR G106+2.7
- LHAASO J1956+2845

LHAASO J1956+2845

Astronomical objects in the field :

- PSR J1954+2826 (X-ray unconstraining upp lim, bright in gamma Fermi-LAT)
- PSR J1958 (X-ray Chandra and gamma Fermi-LAT)
- SNR G65.1+0.6 (radio and Fermi-LAT)
- SNR G66.0-0.0 (Halpha)
- No evidence for X- or gamma-ray PWN

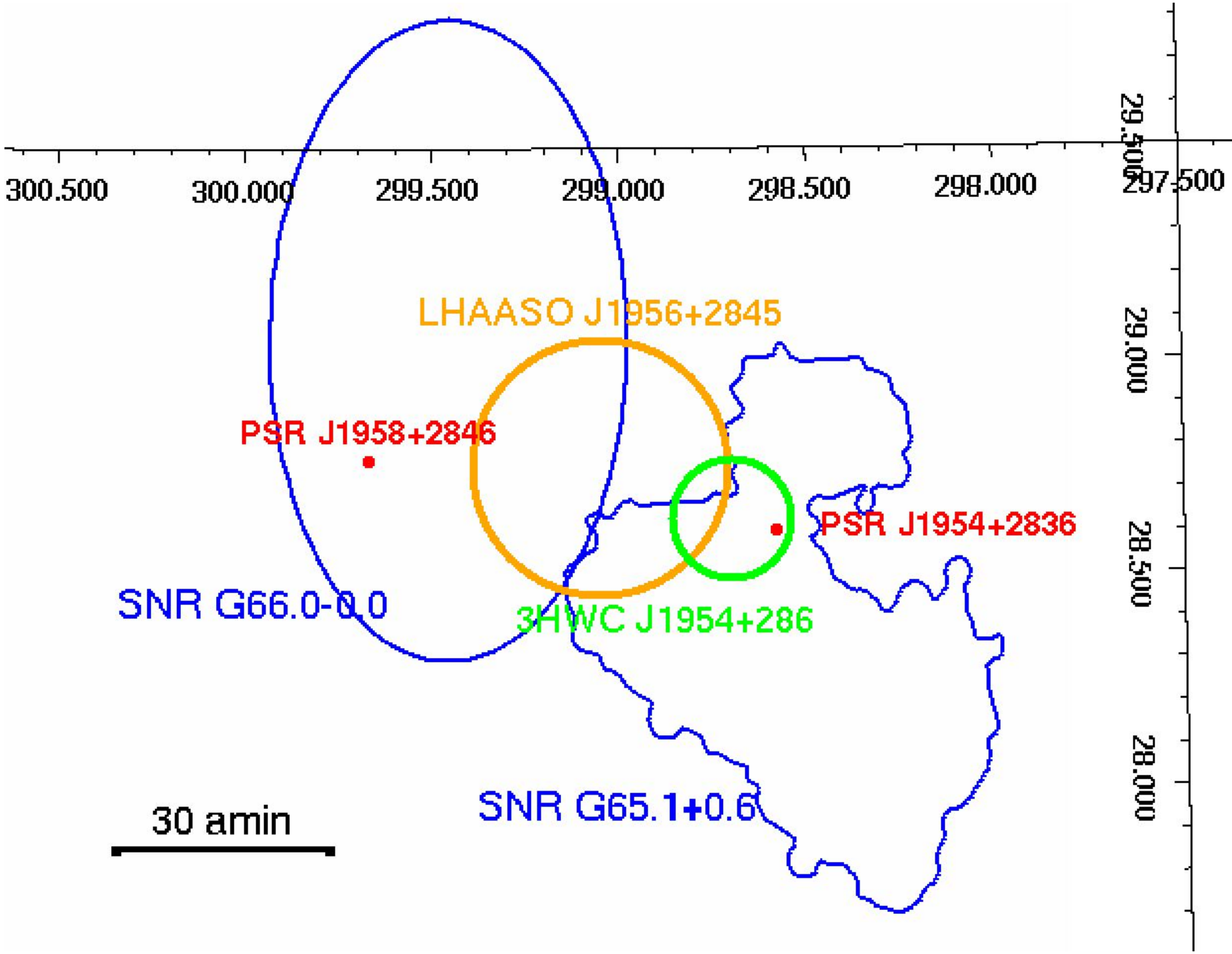

See :
Ackermann et al. 2011, ApJ 726, 35
Kargaltsev et al. 2012, ApJS 201, 37
Prinz & Becker 2015, arXiv:1511.07713
Saz Parkinson et al. 2010, ApJ 725, 571
Xing et al. 2022, ApJ 930, 164

TeV sources in the field

Source	R.A.	Decl.	sqrt (TS)	E	Γ	Flux
	deg	deg		TeV		10^{-13} erg/cm^2/s
LHAASO J1956+2845	299.05	28.75	7.4	100		4.0 ± 0.9
MGRO J1954+28	298.61	28.65	4.3	35		7.3 ± 1.7
MGRO J1958+28	299.53	28.80	4.0	35		6.8 ± 1.7
3HWC J1954+286	298.70	28.63	6.9	4.8-119.7	-2.42 ± 0.12	6.4 ±

In our data challenge, we simulated two distinctive sources, centred in the positions of the two pulsars, with a spatial Gaussian distribution, and a log-parabola spectrum.

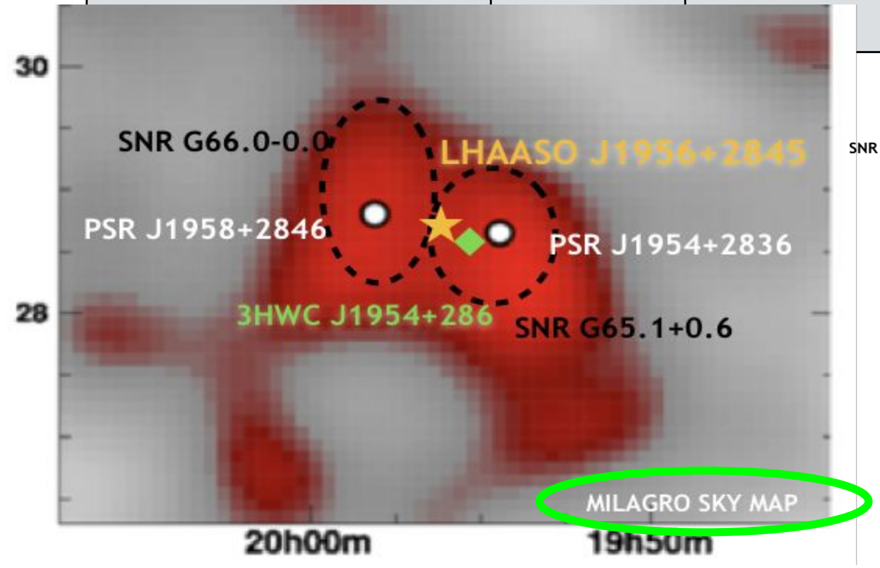

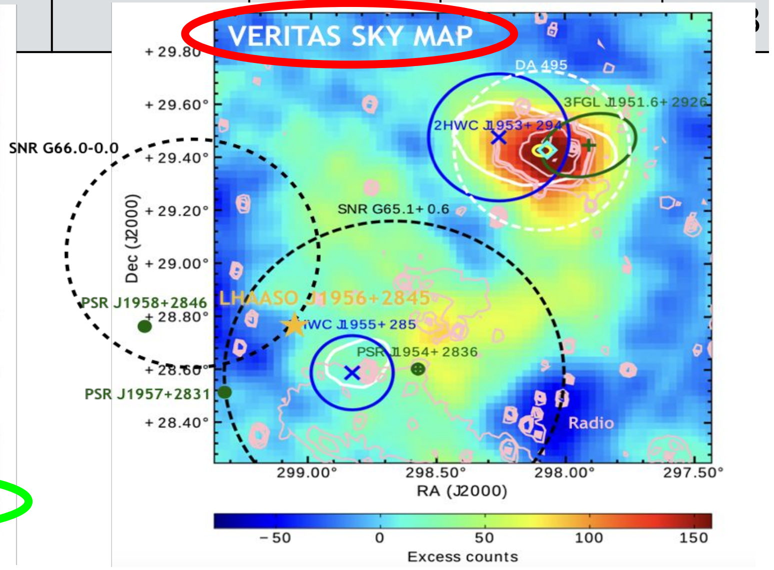

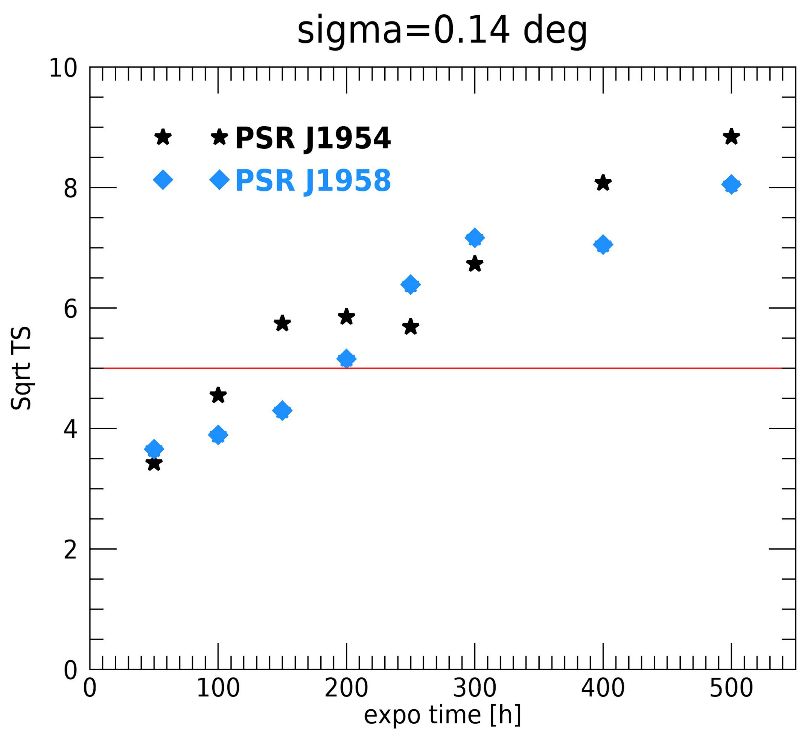

ASTRI Mini-Array - Schedule

June 2022

Phase 0

- 1 Telescope Structure
- m-ICT

Spring 2023

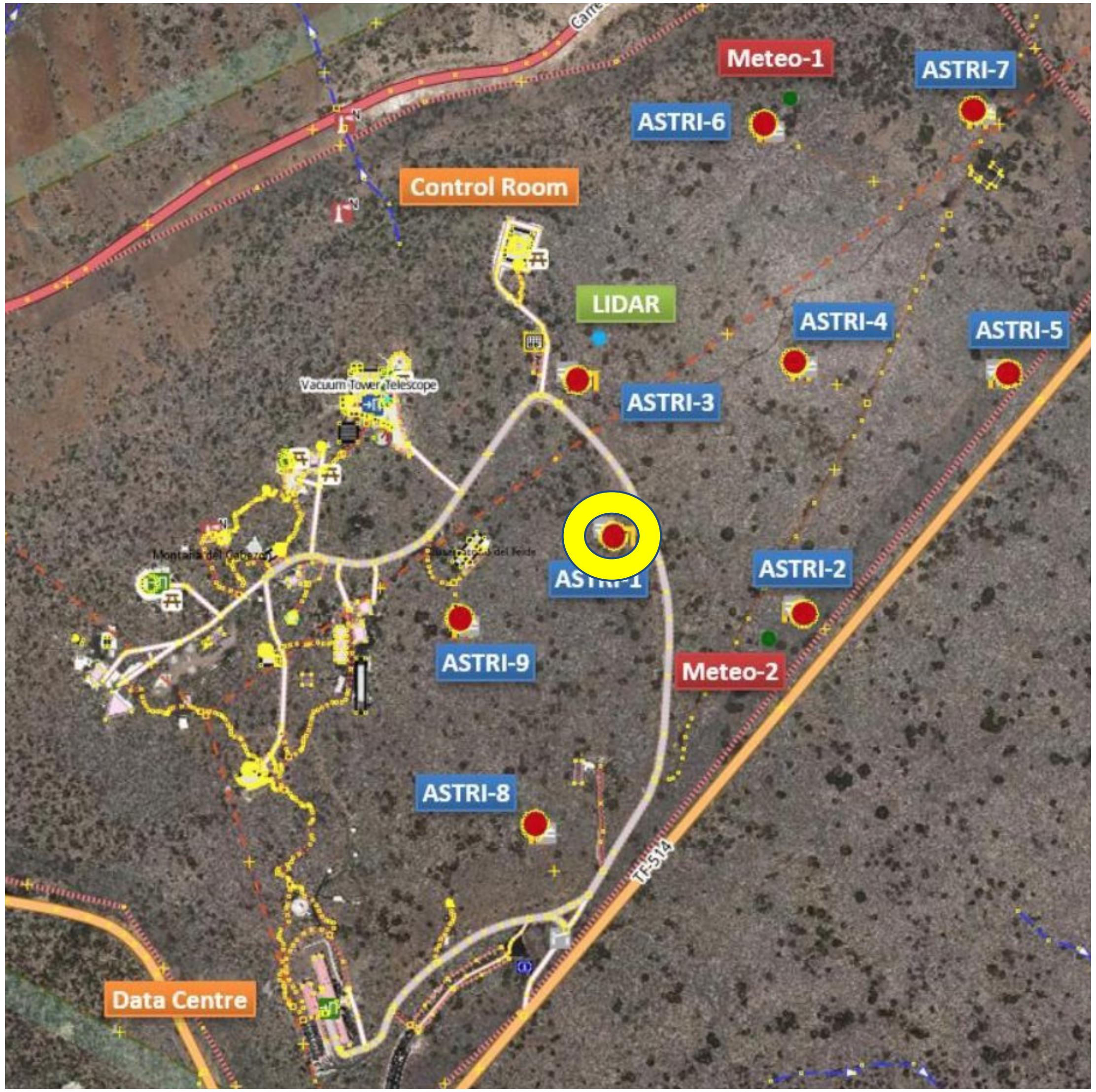

ASTRI Mini-Array - Schedule

June 2022

Phase 0
- 1 Telescope Structure
- m-ICT

Spring 2023

Phase 1
- 3 Telescope Structures

Late 2023

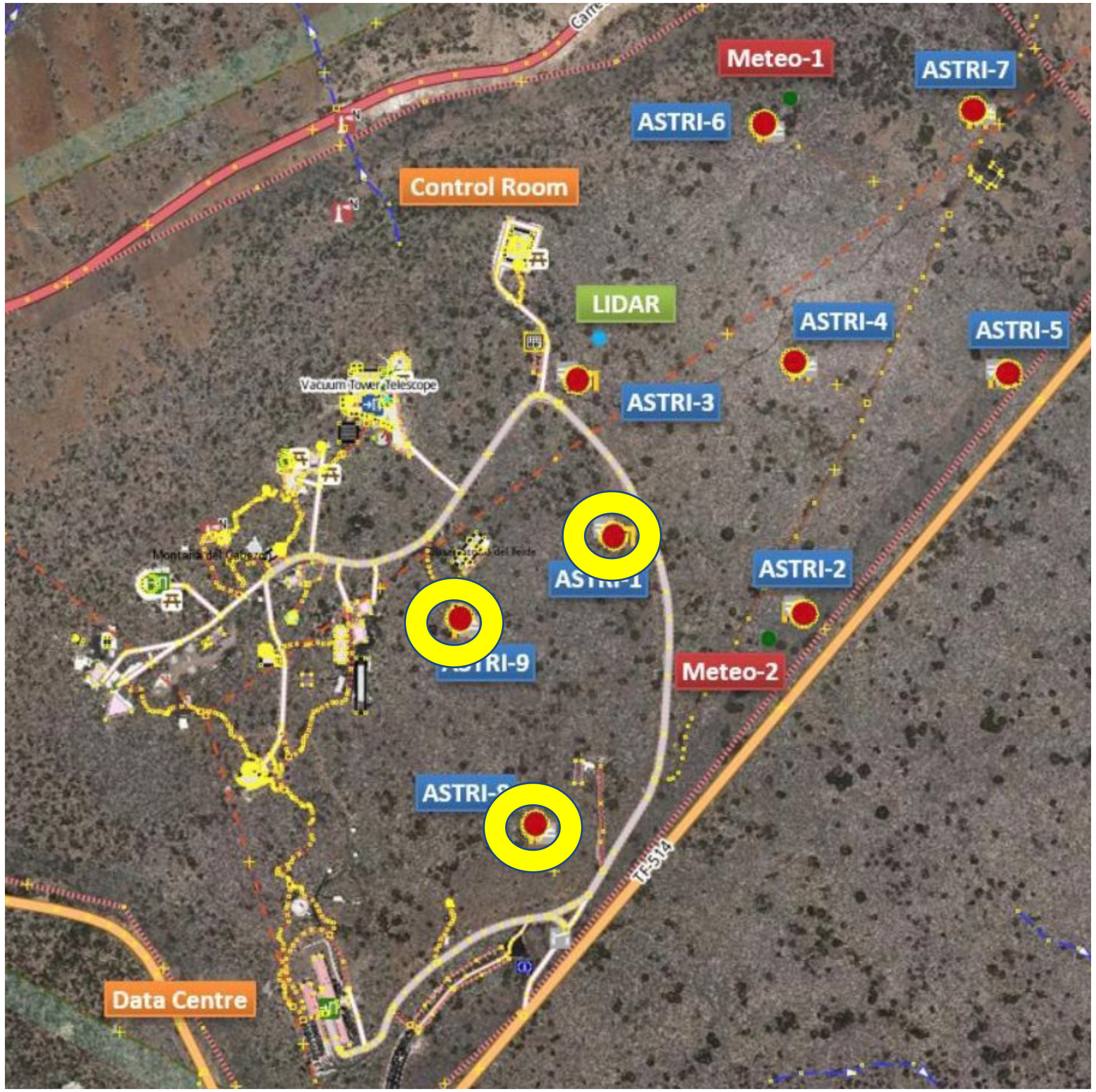

ASTRI Mini-Array - Schedule

June 2022

Phase 0
- 1 Telescope Structure
- m-ICT

Spring 2023

Phase 1
- 3 Telescope Structures

Late 2023

Phase 2
- 3 Telescope Structures + Cameras

Late 2024

Early observations

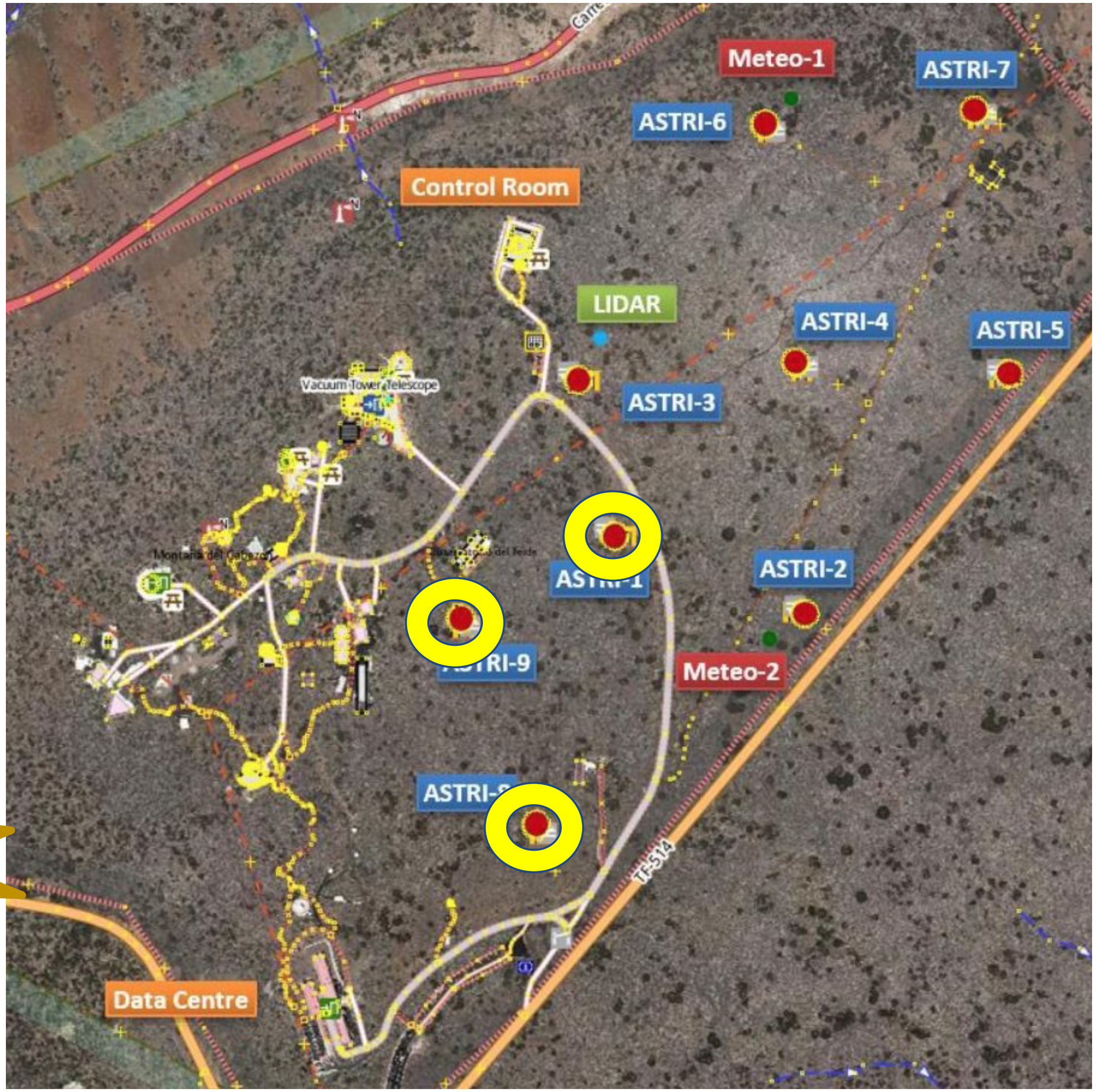

ASTRI Mini-Array - Schedule

June 2022

Phase 0
- 1 Telescope Structure
- m-ICT

Spring 2023

Phase 1
- 3 Telescope Structures

Late 2023

Phase 2
- 3 Telescope Structures + Cameras

Late 2024

Phase 3
- Full Array

Mid 2025

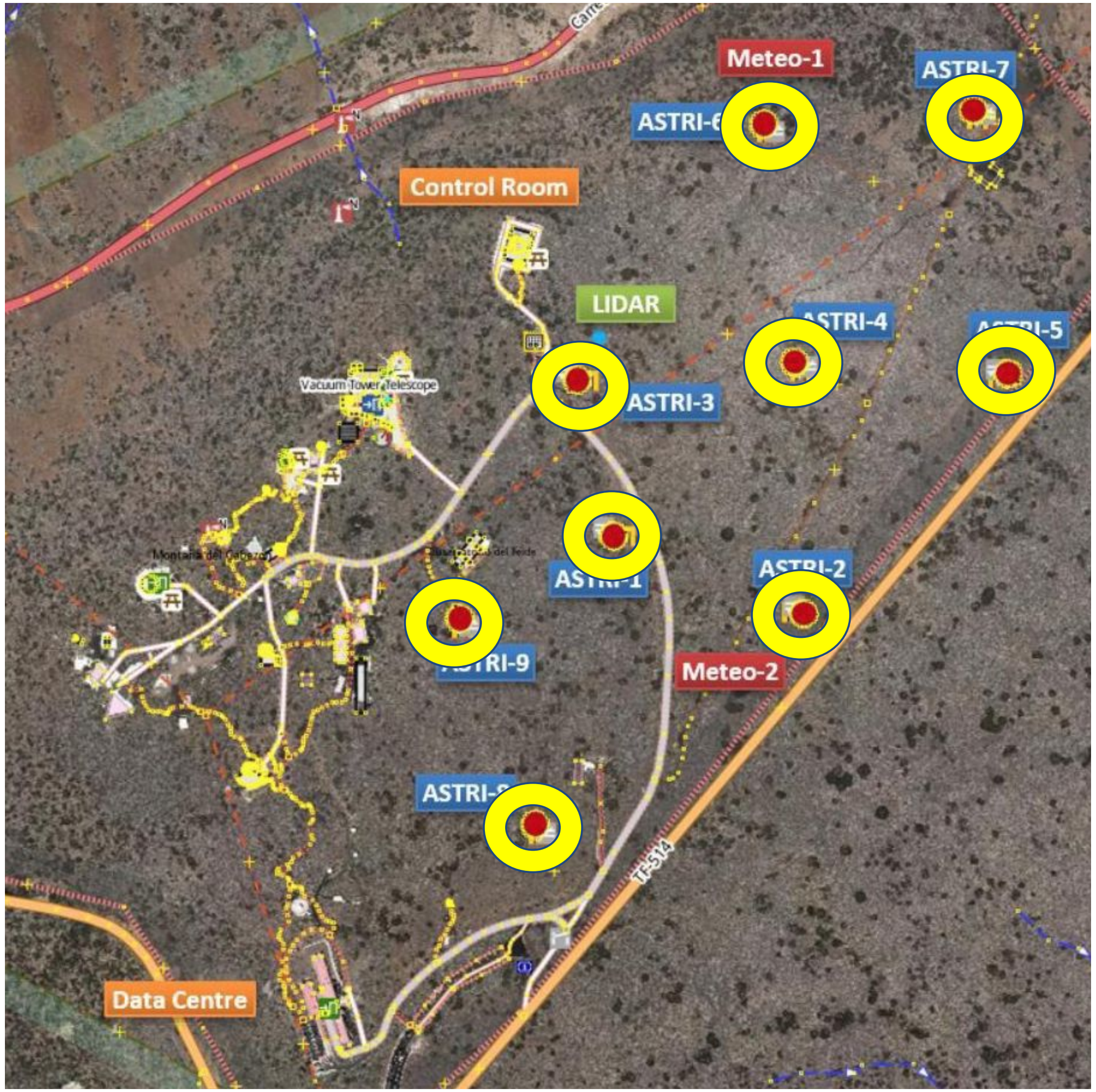

Conclusions

The observing plan will be focused on few (8-12) sky fields :

- ➔ *Large exposures (hundreds of hrs) on the selected sources*
- ➔ *On the Galactic plane we expect many field sources*
- ➔ *observing with half-moon is possible (!) increasing the available time by a factor 1.5*

The ASTRI Mini-Array will investigate with good angular and energetic resolution the most promising PeVatrons candidates

The cygnus region, LHAASO J1908, SNR G106, and other LHAASO sources will be crucial targets in the ASTRI Mini-Array observing strategy

Backup Slides

ASTRI Mini-Array @ Teide Observatory

- Under construction at the Observatorio del Teide (Tenerife), in collaboration with IAC
- Being **developed in all its aspects**, from design/implementation of all HW/SW components to dissemination of final scientific products
- Unprecedented performance and wide FoV for observations at **multi-TeV energy scale**
- **Core Science Program** in the first 3 years
- **Important synergies** with other Northern ground-based gamma-ray facilities (LHAASO, HAWC, MAGIC, VERITAS, CTAO-N)

"Pillar" Sources

from Vercellone et al.

Pillar 1
Origin of CRs

- **PeVatrons**
- **CRs Propagation**
- **Pulsar Wind Nebulae**

Pillar 2
Cosmology and Fund. Physics

Name	Type	Exposure (Hrs)
Tycho Snr	SNR	400
Gal. Center	Diffuse	260
VER J1907	SNR+PWN	500
G106.3+2.7	SNR	200
γ-Cygni	SNR	500
W28	SNR/MC	500
M82	Starburst	400
Crab	PWN	300
Geminga	PWN	500
IC 310	Radio gal	10-500
M87	Radio gal	10-500
Mkn 501	Blazar	5-500
1ES 0229+200	Blazar	200-250

“Pillar” Sources

from Vercellone et al.

Pillar 1
Origin of CRs

- **PeVatrons**
- **CRs Propagation**
- **Pulsar Wind Nebulae**

Pillar 2
Cosmology and Fund. Physics

Name	Type
Tycho Snr	SNR
Gal. Center	Diffuse
VER J1907	SNR+PWN
G106.3+2.7	SNR
γ-Cygni	SNR
W28	SNR/MC
M82	Starburst
Crab	PWN
Geminga	PWN
IC 310	Radio gal
M87	Radio gal
Mkn 501	Blazar
1ES 0229+200	Blazar

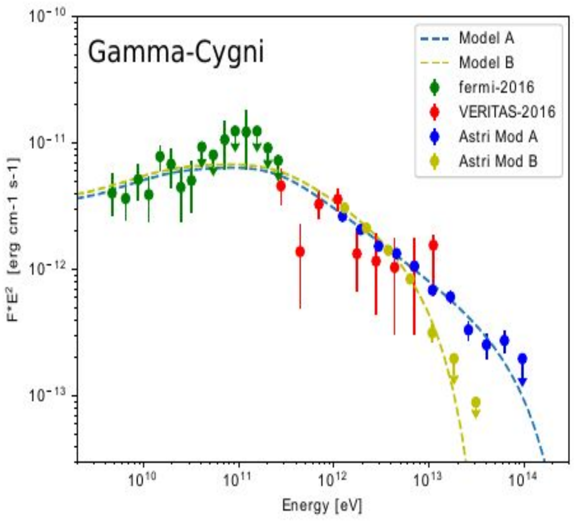

Figure 15: γ-ray spectrum of γ-Cygni. Data are from Fermi-LAT and VERITAS while theoretical models A and B (described in the text) are showed with dashed curves. Blue and yellow dots show the ASTRI Mini-Array simulations for model A and B, respectively, for 500 hr of exposure.

Observing Plan : an example

Per year :

Moonless Night Hours	1565
Fraction of clear nights (<20% cloud)	0,79
Loss due to bad weather	0,04
Loss due to "Calima"	0,07
Average Annual Observation Time	1100

Availability: 91%
Uptime: 1000 h
Downtime 100 h
Mean Dead Time: 20 h
5 Failures at system level per year

Duty Cycle: 13% defined as AAOT/Hours yr

on 3 years : 3300 -3000 hours (moonless)

Time budget (Hrs):

Pillar 1 2000

- Pevatrons 1000
- CRs diffusion 500
- PWNe 500

Pillar 2 1300

Observing Plan : an example

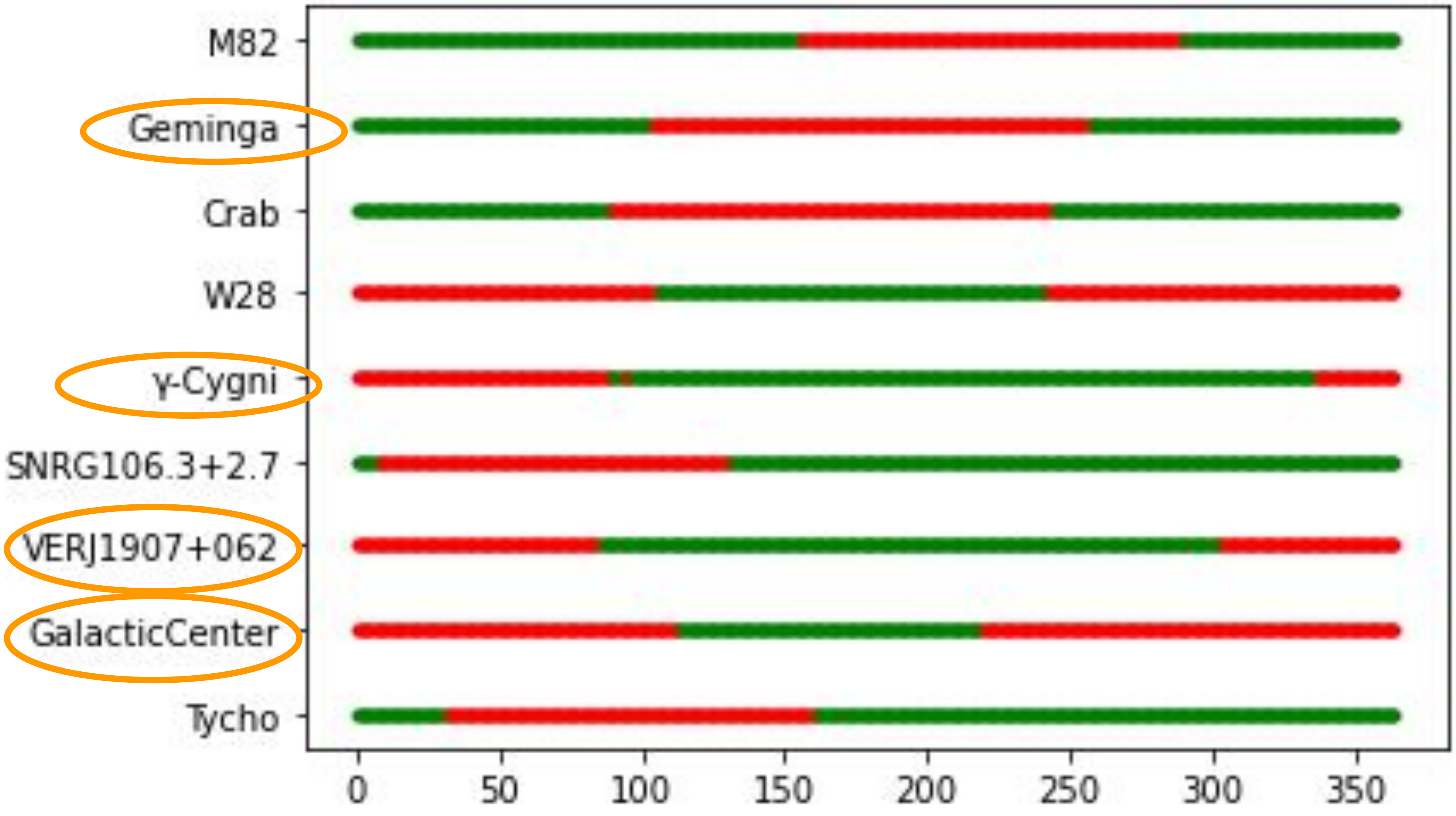

plus :

IC 310

Mrk 501

Observing Plan . Visibility in 2024

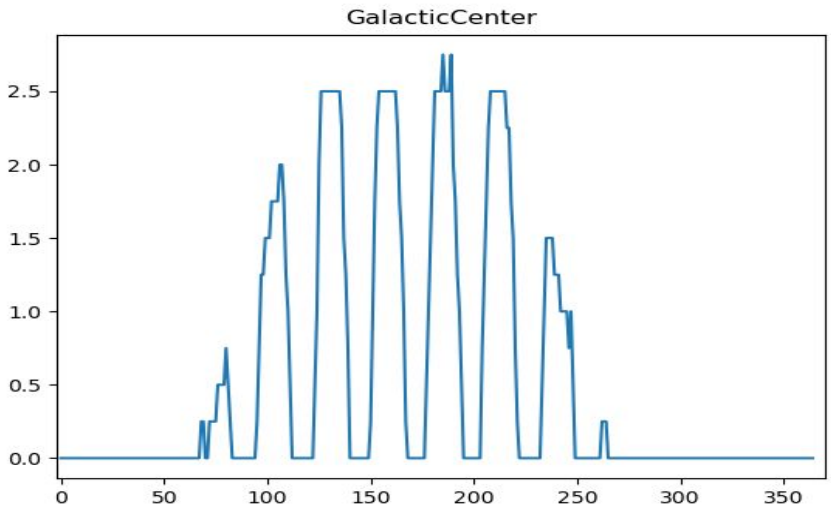

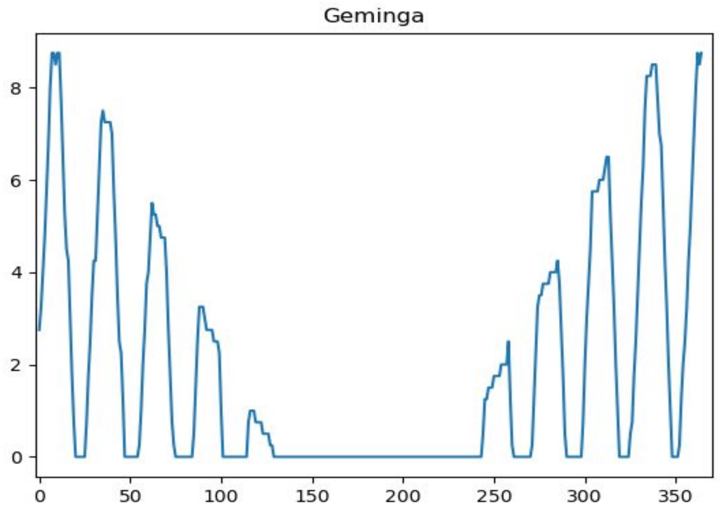

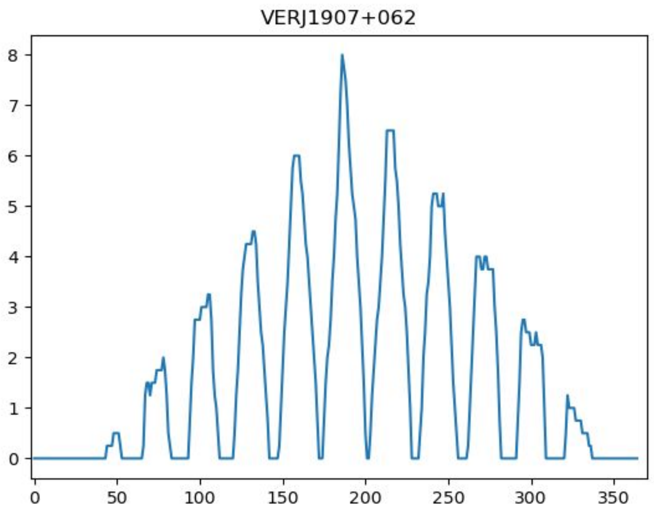

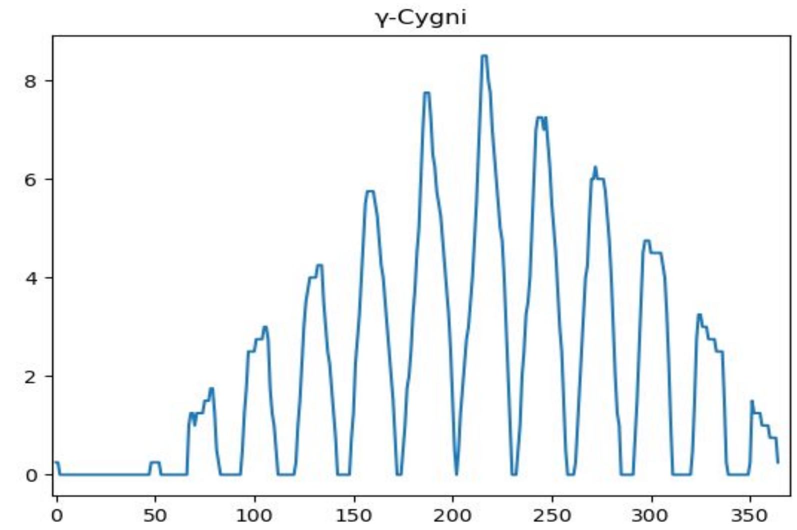

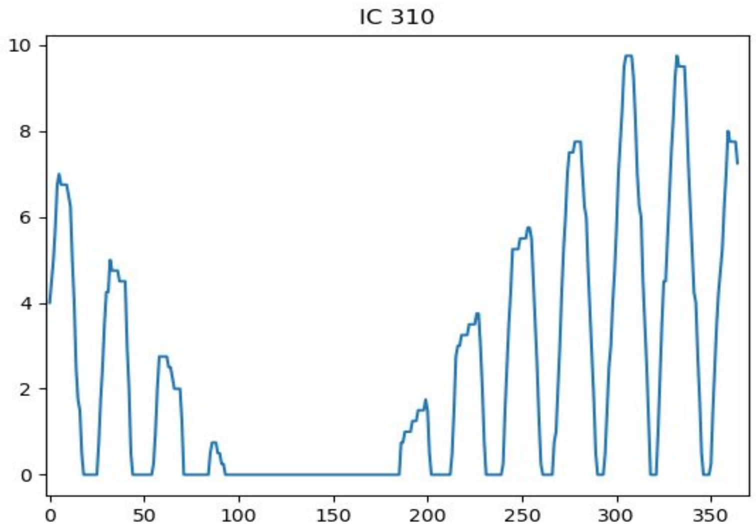

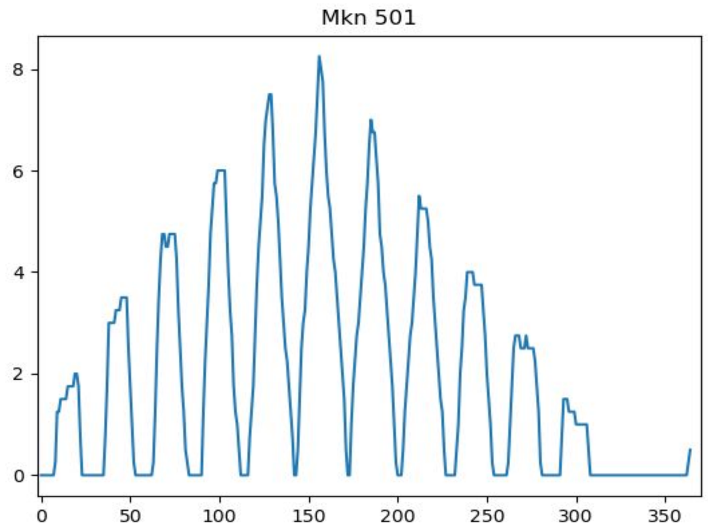

Observing Plan

Hours per year (2024) :

Geminga :	*148.25*
Mkn 501 :	*144.5*
g-Cygni (1) :	*26.75*
Gal Center :	*138.0*
VER J1907+062 :	*142.5*
g-Cygni (2) :	*91.75*
IC 310 :	*180.0*

Over 3 years :

P1 :	**1641.75**
Pevatrons :	841.5
CRs diffusion :	355.5
PWNe :	444.75
P2 :	**973.5**

Time budget :

Pillar 1 2000

- Pevatroni 1000
- CRs diffusion 500
- PWNe 500

Pillar 2 1300

Observing Plan - MoonLight (CTA)

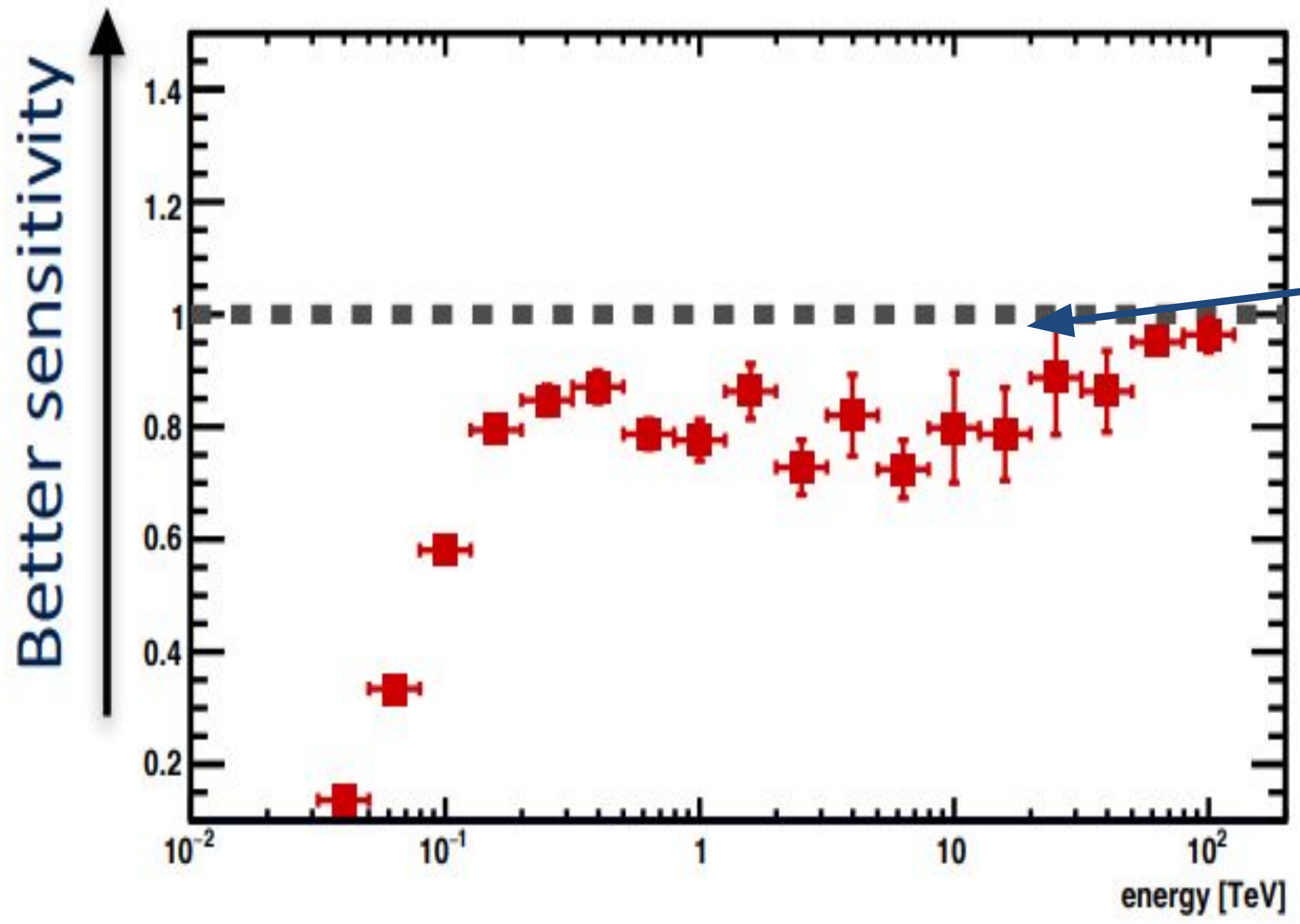

Little degradation above ~ 10 TeV

MoonLight

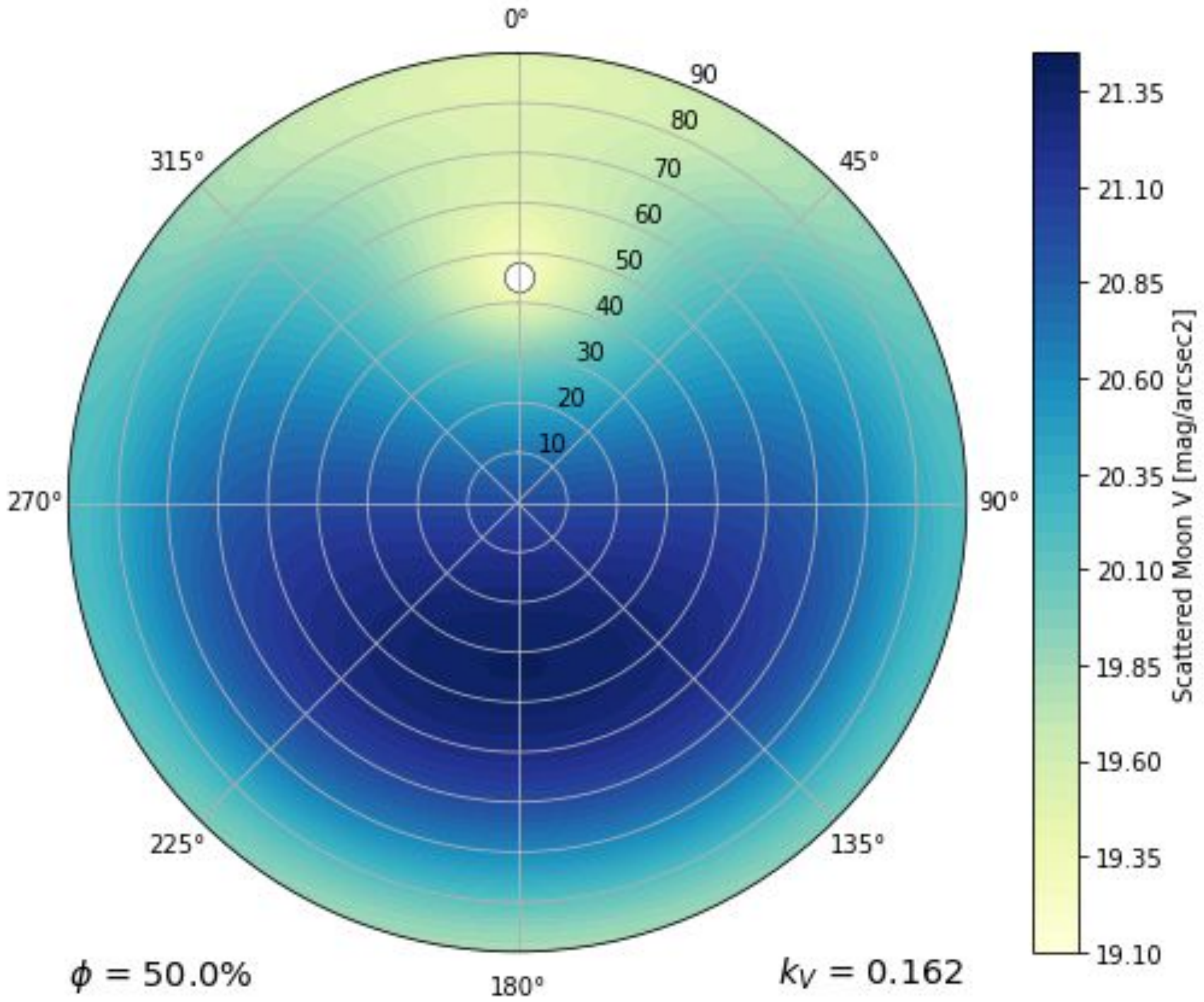

- SpecSim
  (https://specsim.readthedocs.io)
- Based on the model by ***Krisciunas&Schaefer***

Brightness in V [mag/arcsec^2]

	SkyCalc	SpecSim	diff Fluxes
halfmoon_sep20	*20.04*	*20.03*	*0.9 %*
halfmoon_sep40	*20.47*	*20.52*	*4.7 %*
halfmoon_sep60	*20.68*	*20.75*	*6.7 %*
fullmoon_sep40	*18.33*	*18.30*	*2.8 %*

Observing under MoonLight

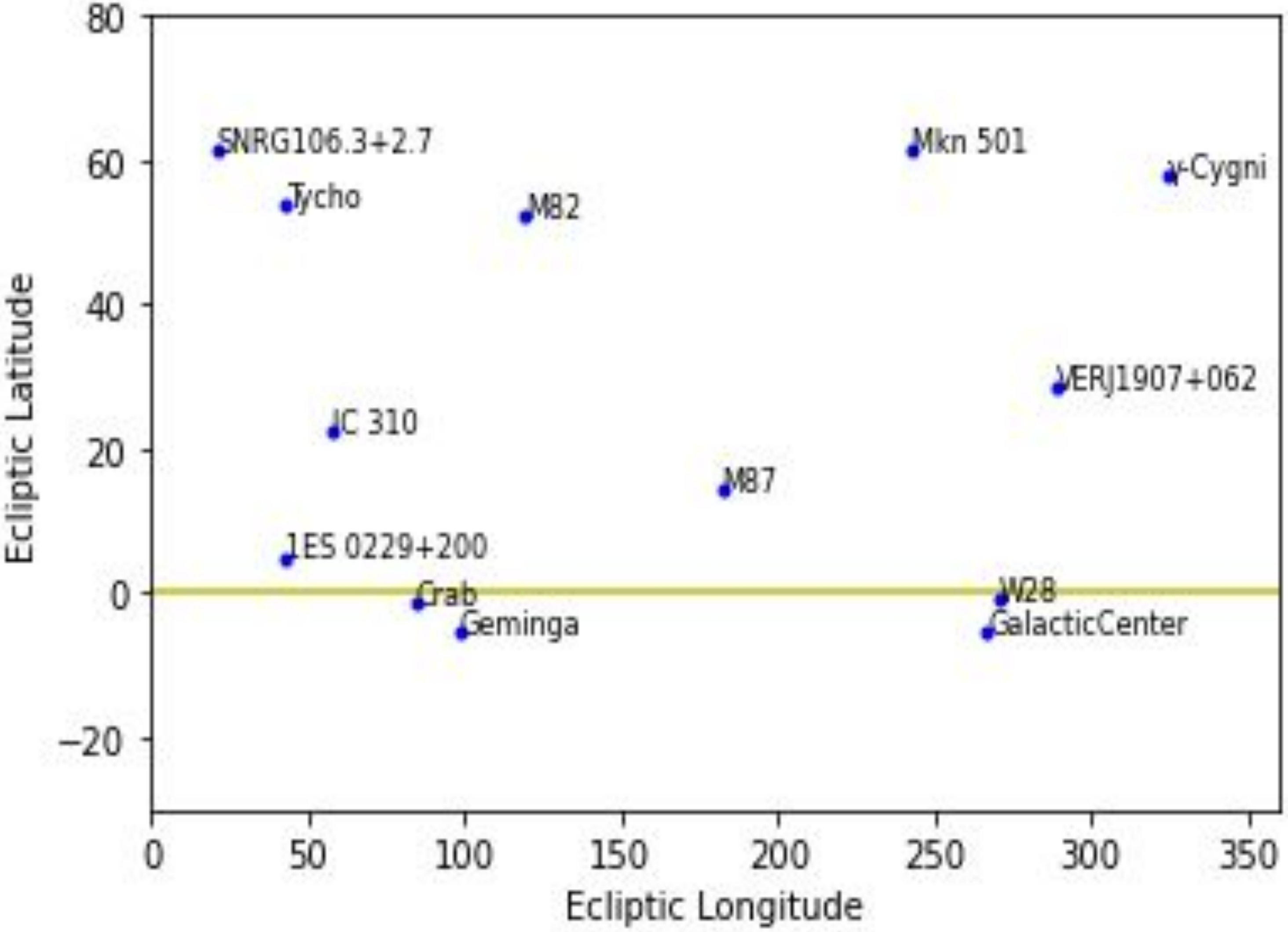

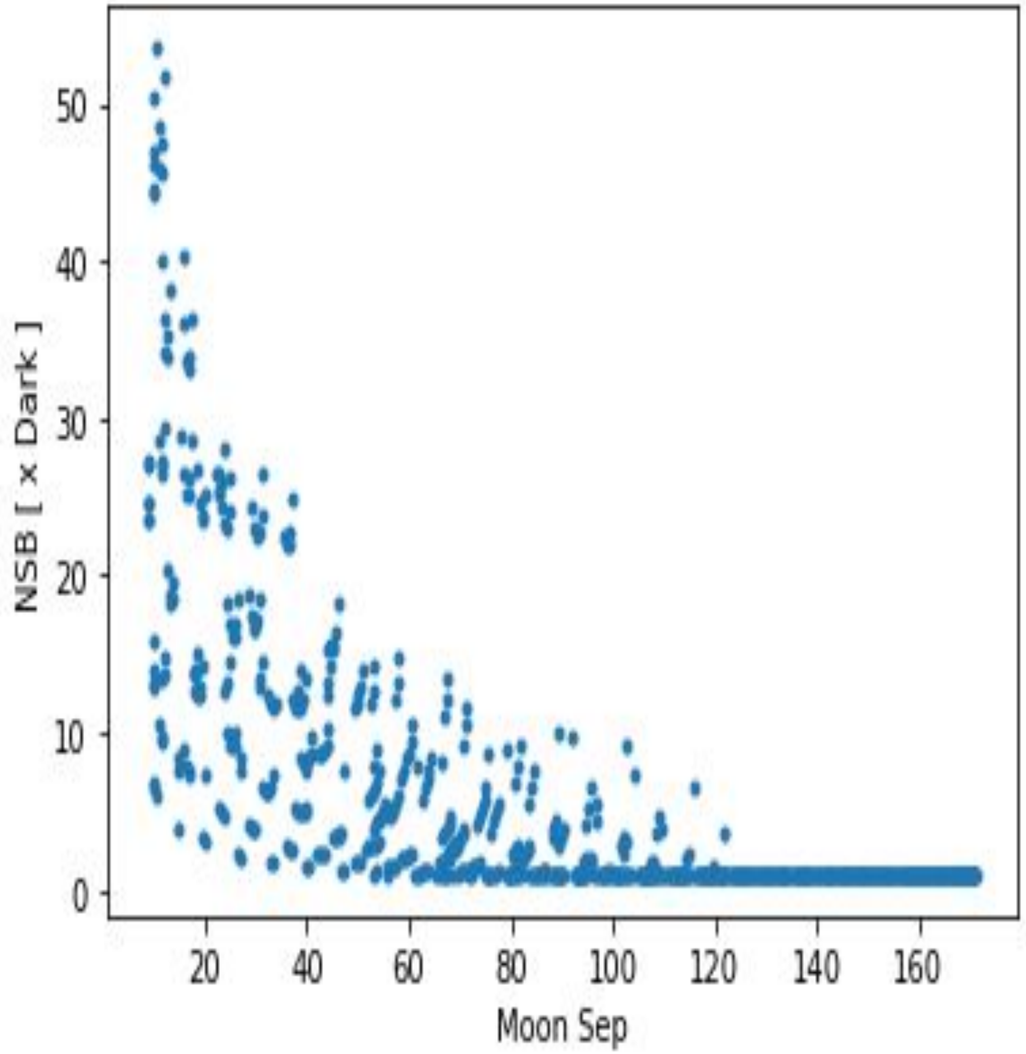

Observing Plan - MoonLight - Geminga Halo

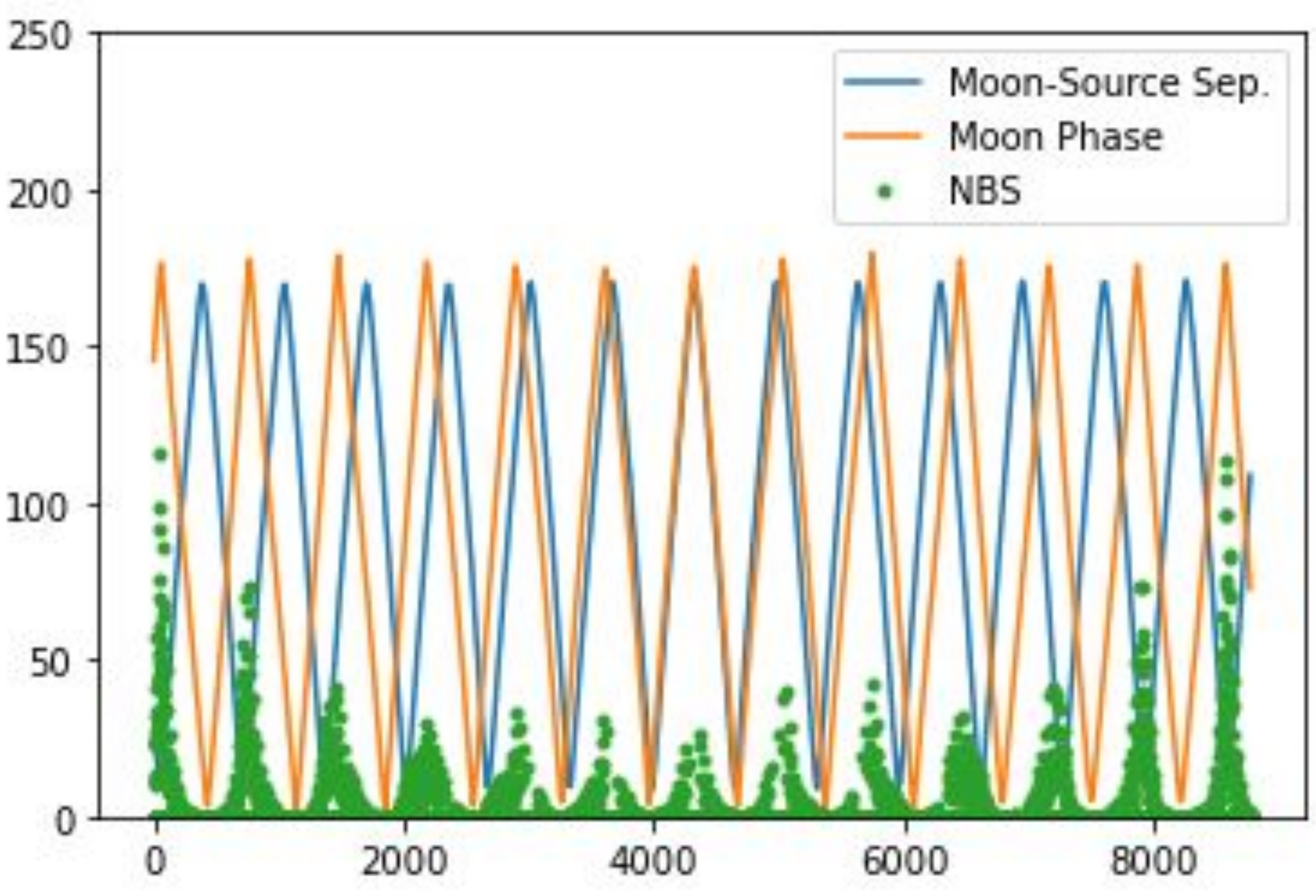

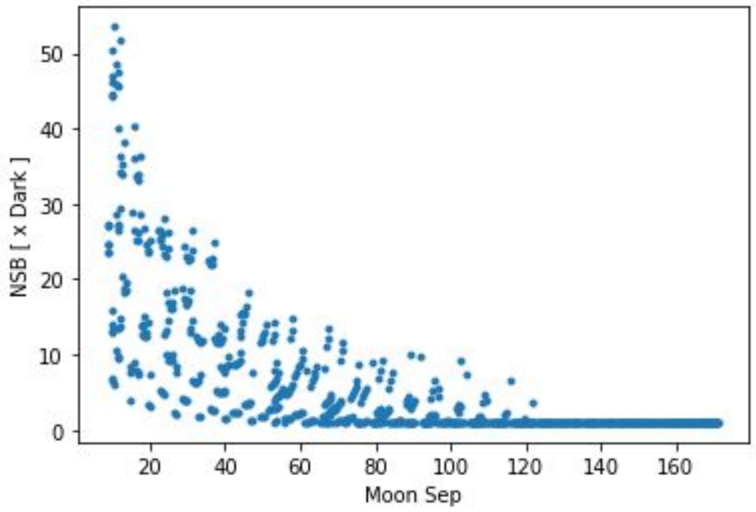

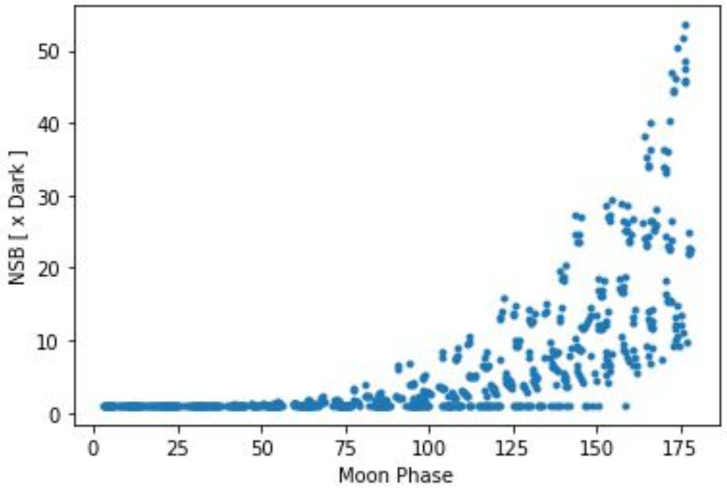

- For year 2026
- Dark : $m_V = 21.55$

Observing Plan - MoonLight - Geminga Halo

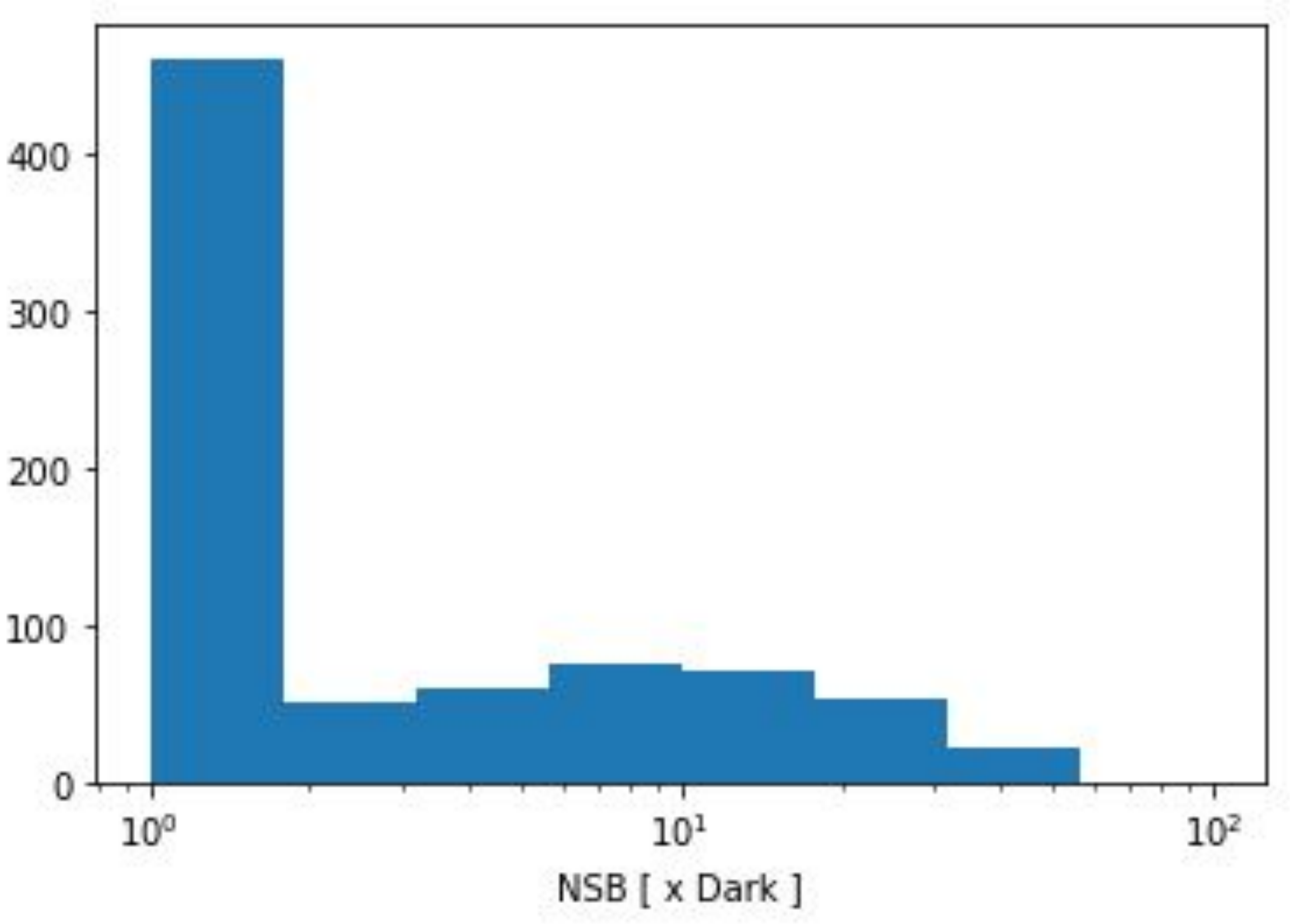

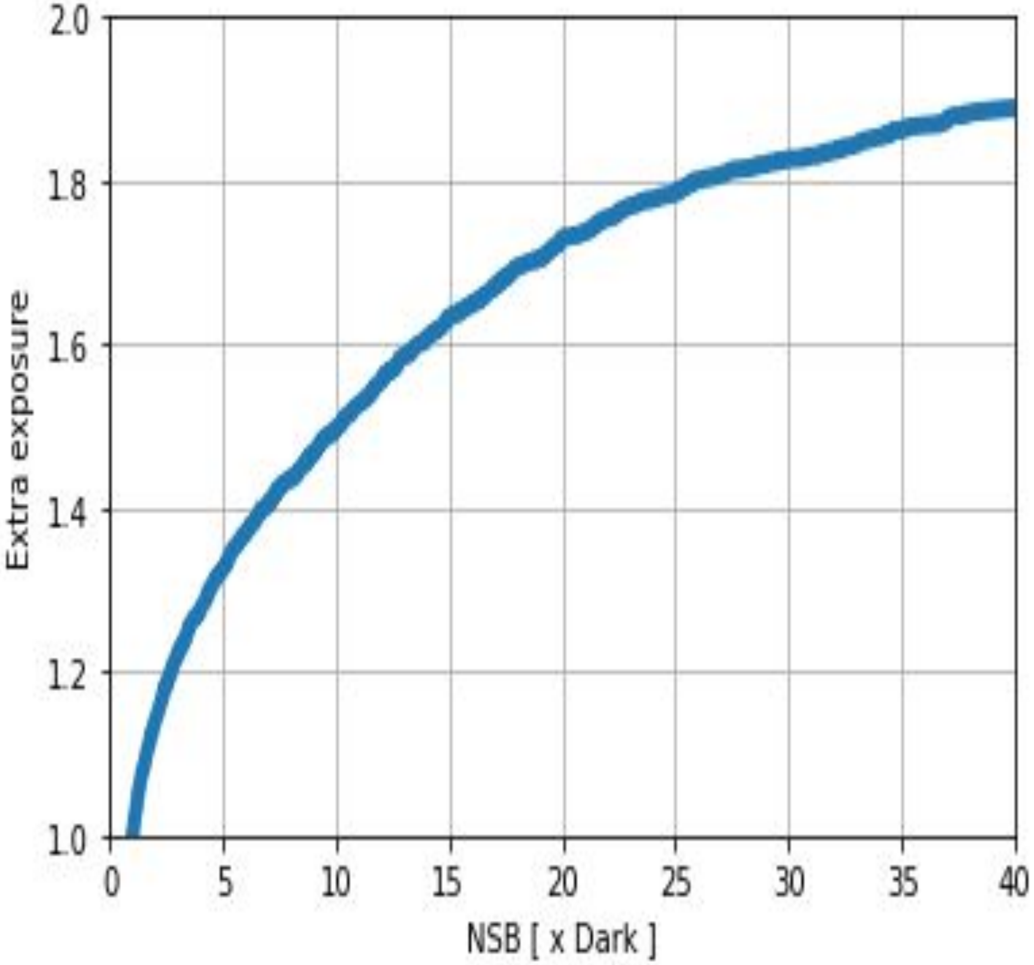

Observing under MoonLight

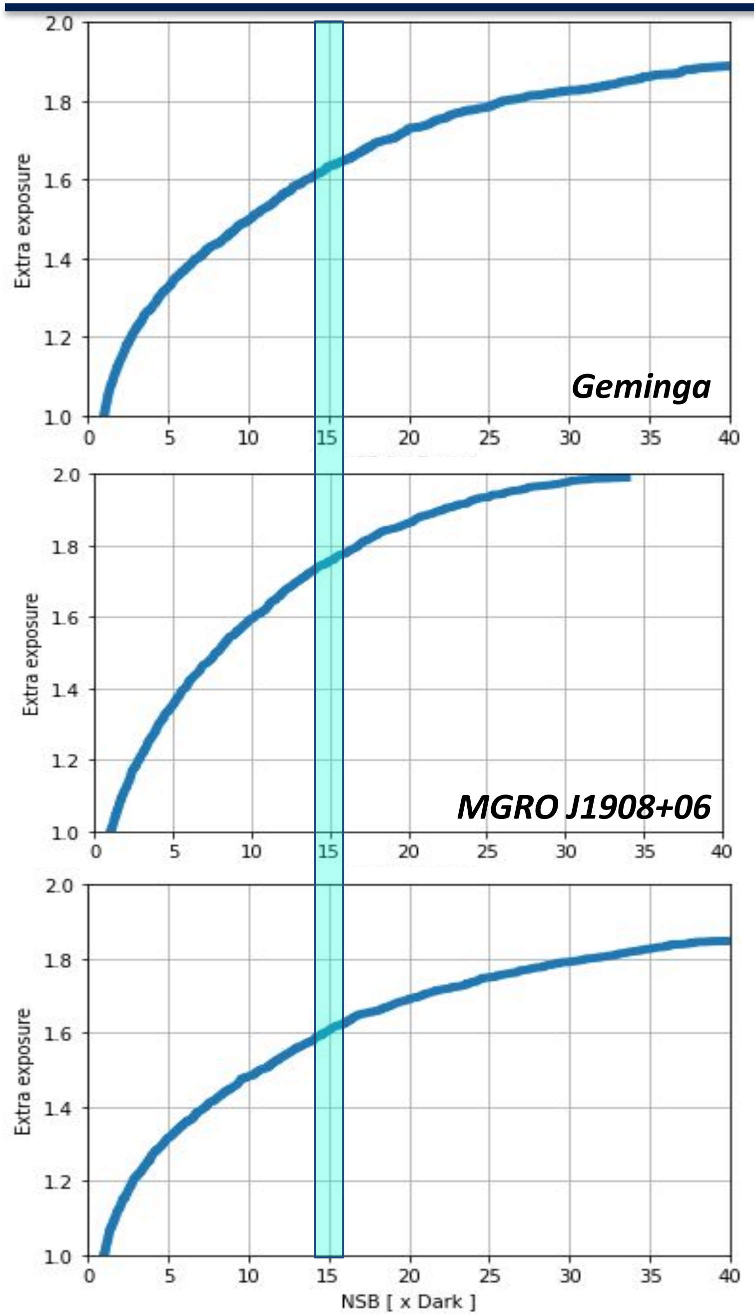

Dark NSB : ***0.24 ph / cm² ns sr***

in the band 300-650 nm

15 x Dark NSB : ***3.6 ph / cm² ns sr***

corresponding to : ***~ 1 GHz*** *on one camera pixel*

~ 50-70 %

Observing Plan - Large FOV → sec. targets

Lot of TeV sources in the Observing-Plan fields, for example :

GC ……………………….. SNR G0.9+0.

VERJ1907 ……………... W 49B,

SS 433,

2HWC J1902+048

gamma-Cygni ……... 2HWC J2024+417

Geminga ………………… IC 443

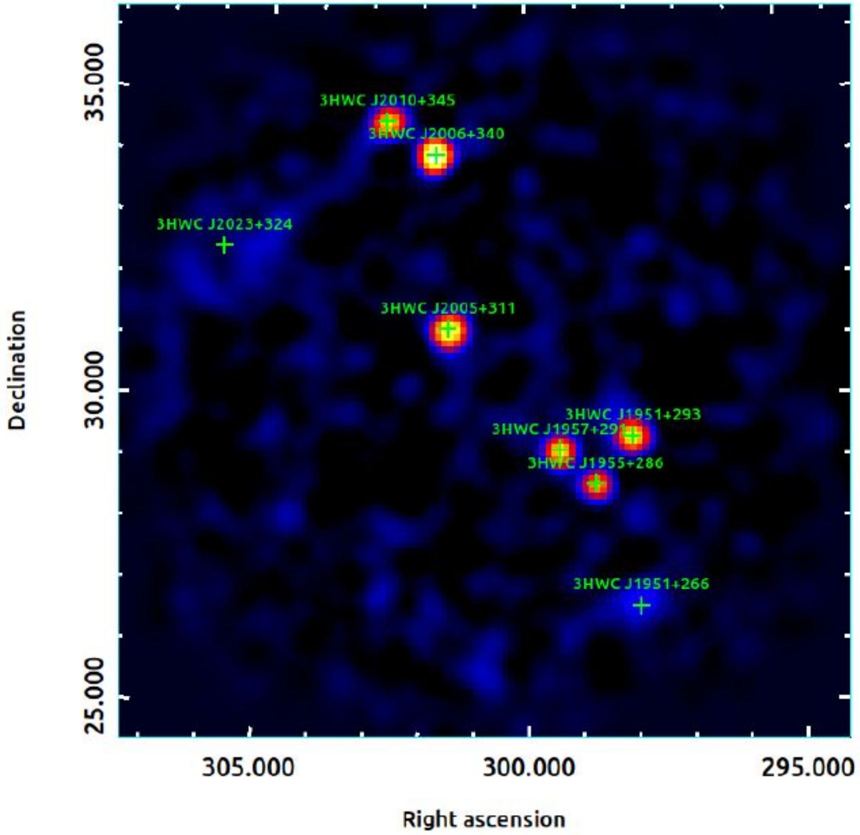

Figure 13: ASTRI Mini-Array 200 hr simulation of the Cygnus Region. Green crosses mark the positions of the 3HWC sources in a 10° × 10° field of view (see text for details).

ASTRI - LHAASO synergies

ASTRI will be able to characterize the LHAASO sources with good angular and spectral resolution

LHAASO observations can help ASTRI to choose the best targets on the sky to observe with deep exosures

Follow up of LHAASO sources : the case of J1908+0621

ASTRI Mini-Array **200 hr simulation (up to E~200 TeV)** of [2HWC J1908+063]

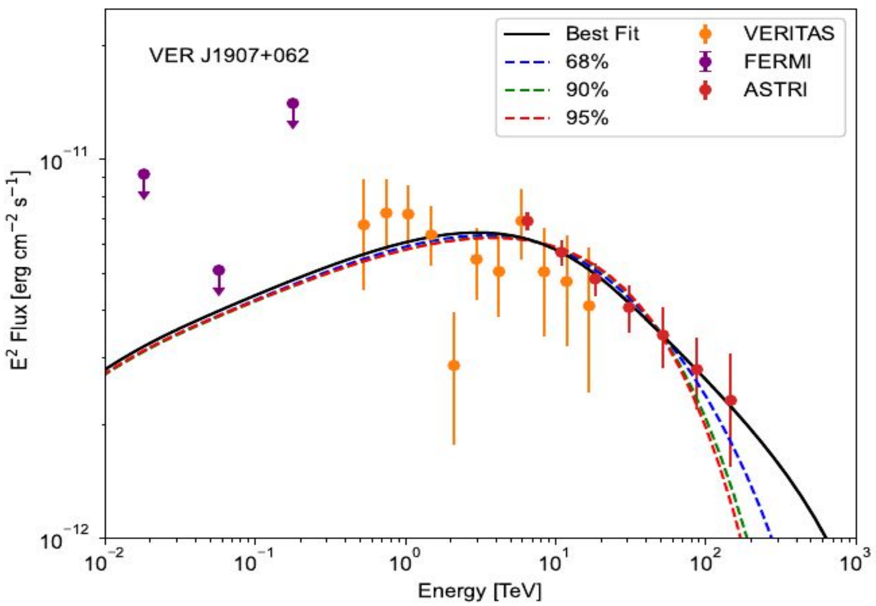

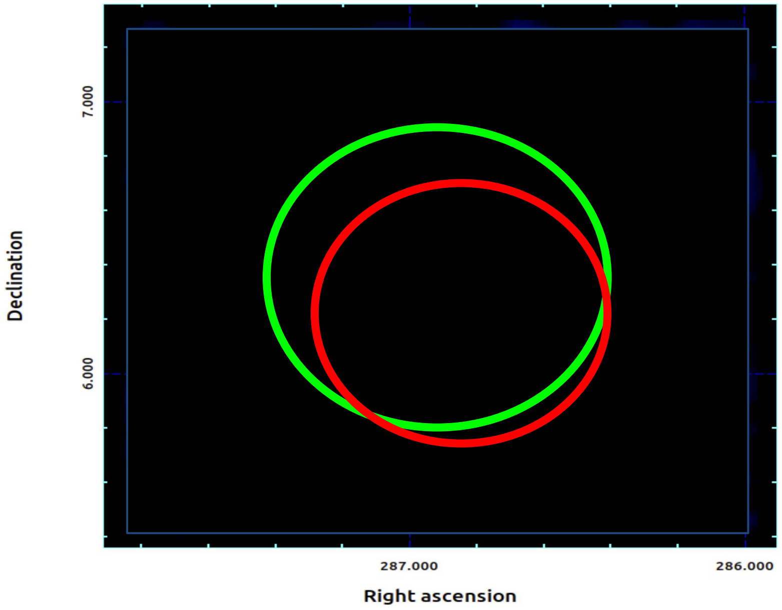

The light green circle marks the ~ 0.52° HAWC error-box

VER 2016+361 -

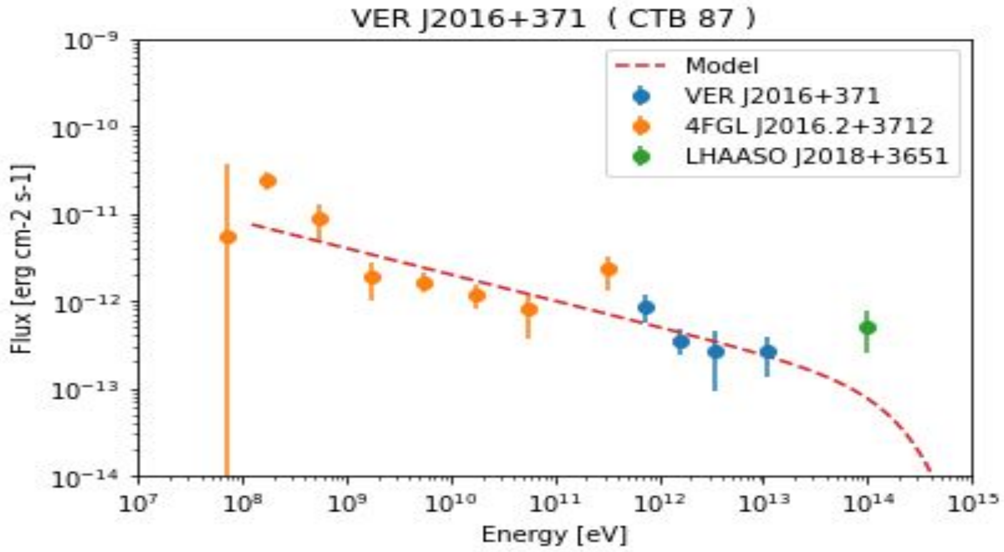

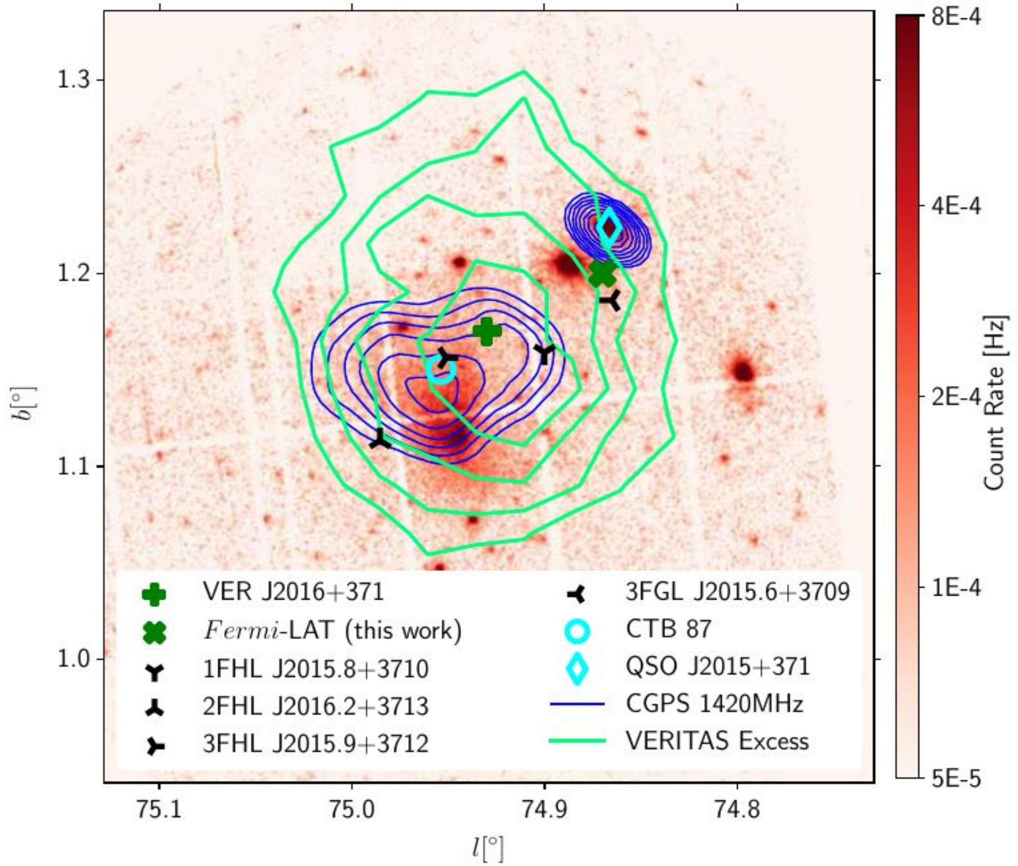

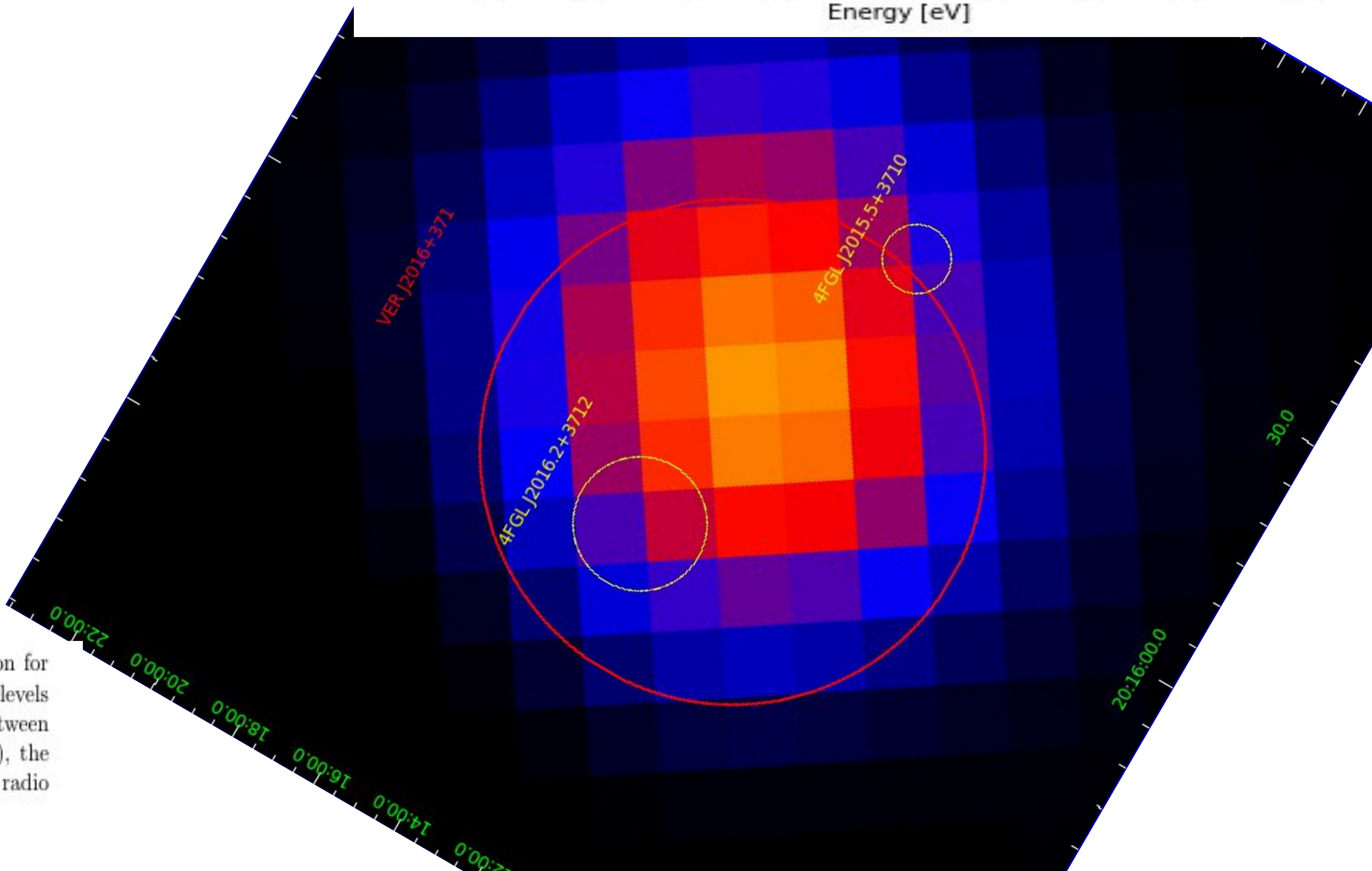

Figure 17. *XMM-Newton* counts (red color scale, observation id. 0744640101, no background subtraction nor correction for variation in exposure across the FoV has been applied). VERITAS excess with the *Point* integration region is shown in levels of ten counts starting at 30 (bright green) along with CGPS 1420 MHz contours (eight logarithmically spaced levels between brightness temperatures 20 and 150 K (Taylor et al. 2003), dark blue). The locations of VER J2016+371 (green plus), the *Fermi*-LAT position from this work (green cross) and the positions from the different catalogs (black tri symbols) and the radio locations of CTB 87 (cyan o) and QSO J2015+371 (cyan diamond) are shown for comparison.

VER 2020+368

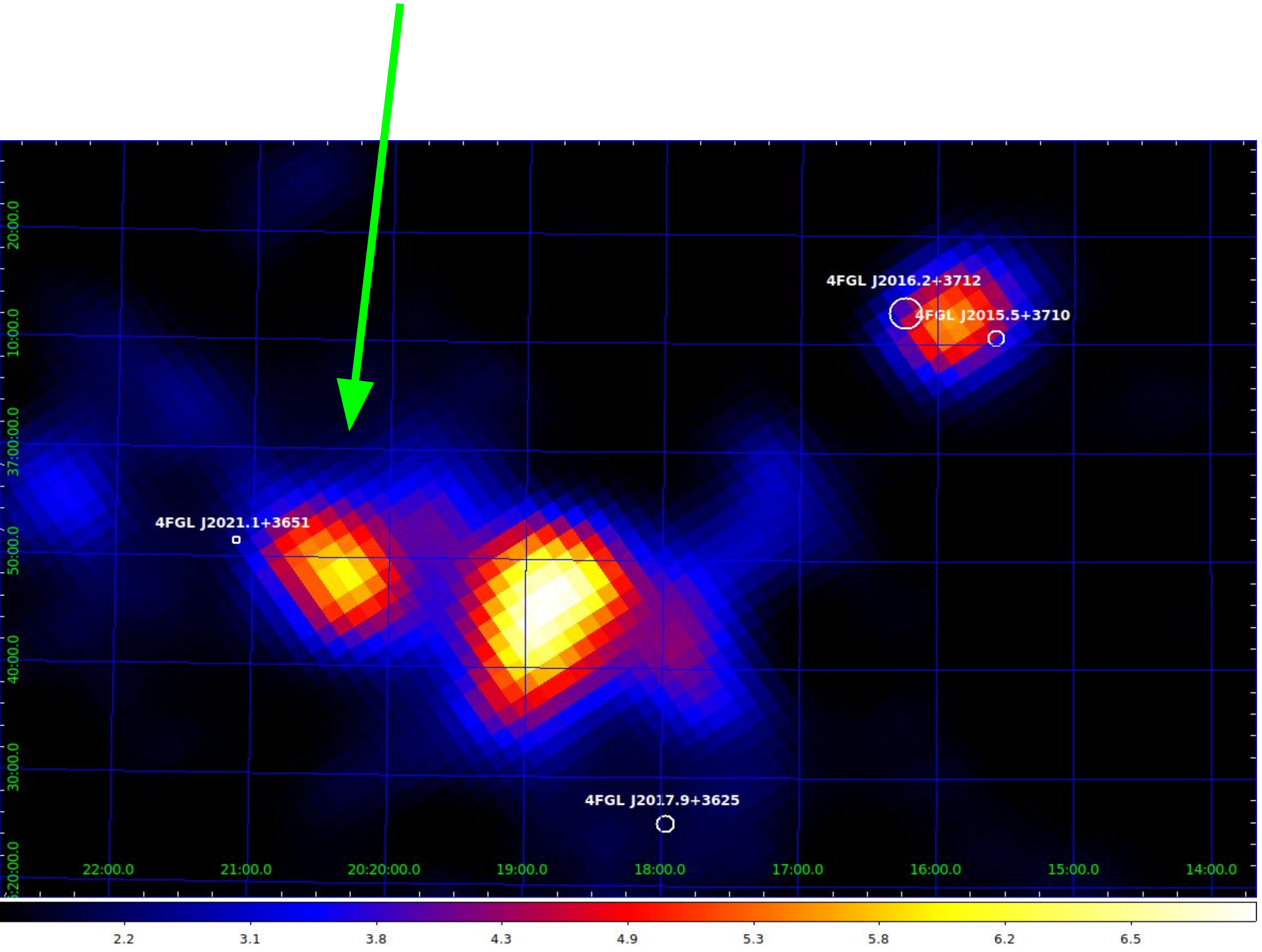

4FGL J2016.2+3712
4FGL J2015.5+3710
4FGL J2021.1+3651
4FGL J2017.9+3625
22:00.0
21:00.0
20:20:00.0
19:00.0
18:00.0
17:00.0
16:00.0
15:00.0
14:00.0
20:00.0
10:00.0
37:00:00.0
50:00.0
40:00.0
30:00.0
2.2
3.1
3.8
4.3
4.9
5.3
5.8
6.2
6.5

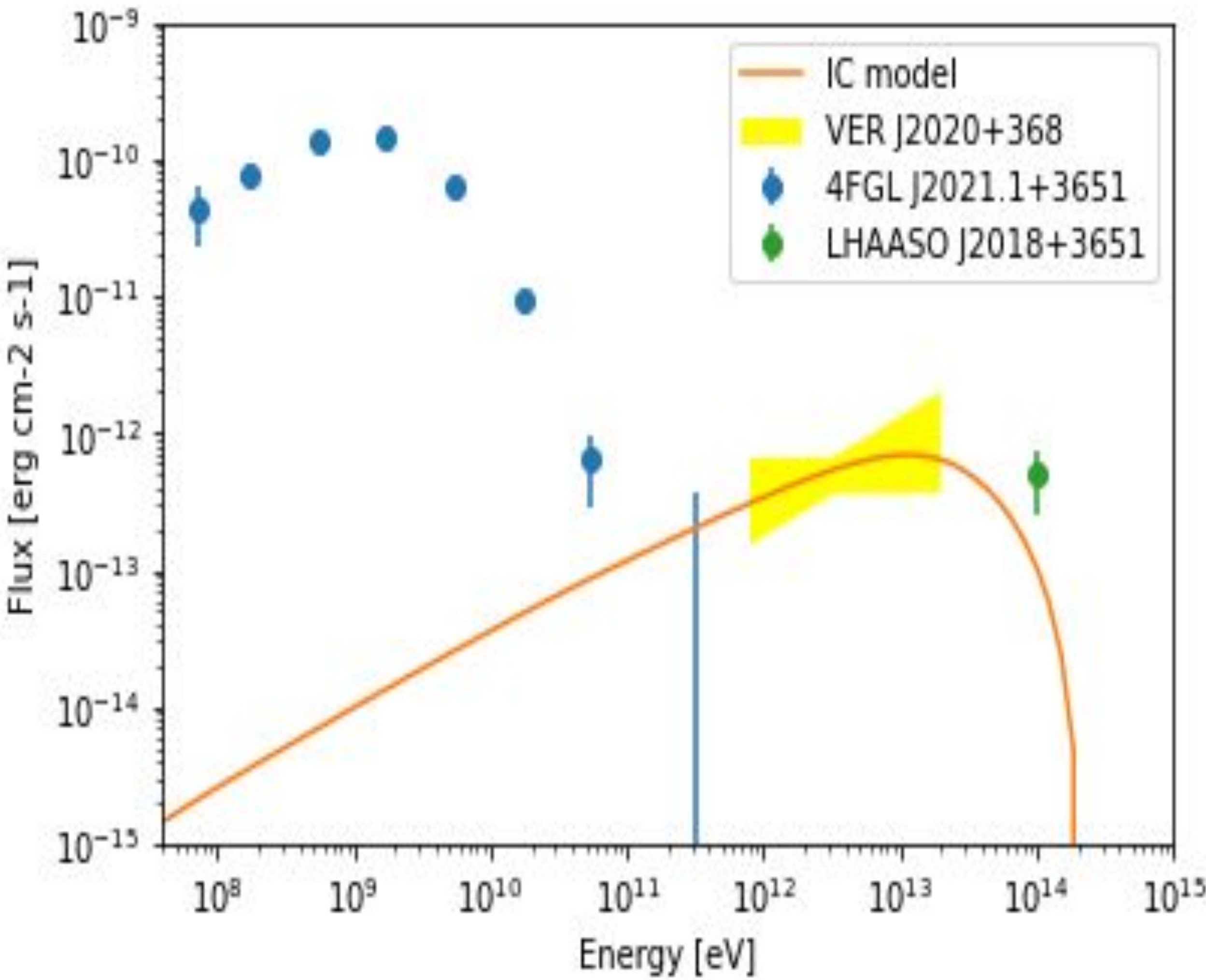

IC model
VER J2020+368
4FGL J2021.1+3651
LHAASO J2018+3651
Flux [erg cm-2 s-1]
Energy [eV]
10^{-9}
10^{-10}
10^{-11}
10^{-12}
10^{-13}
10^{-14}
10^{-15}
10^{8}
10^{9}
10^{10}
10^{11}
10^{12}
10^{13}
10^{14}
10^{15}

VER 2020+368

Mizuno et al.
The Astrophysical Journal, 841:104 (14pp), 2017 June 1

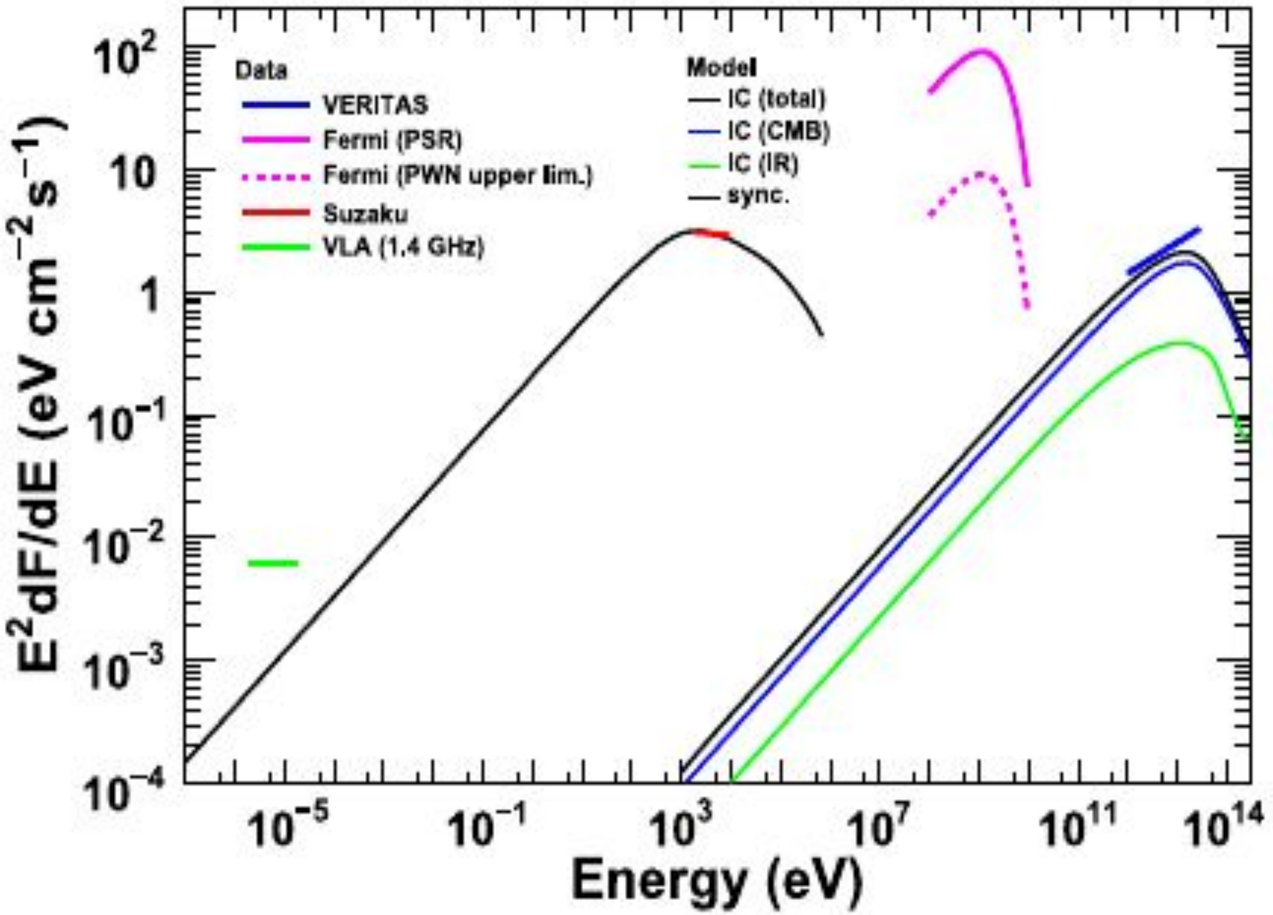

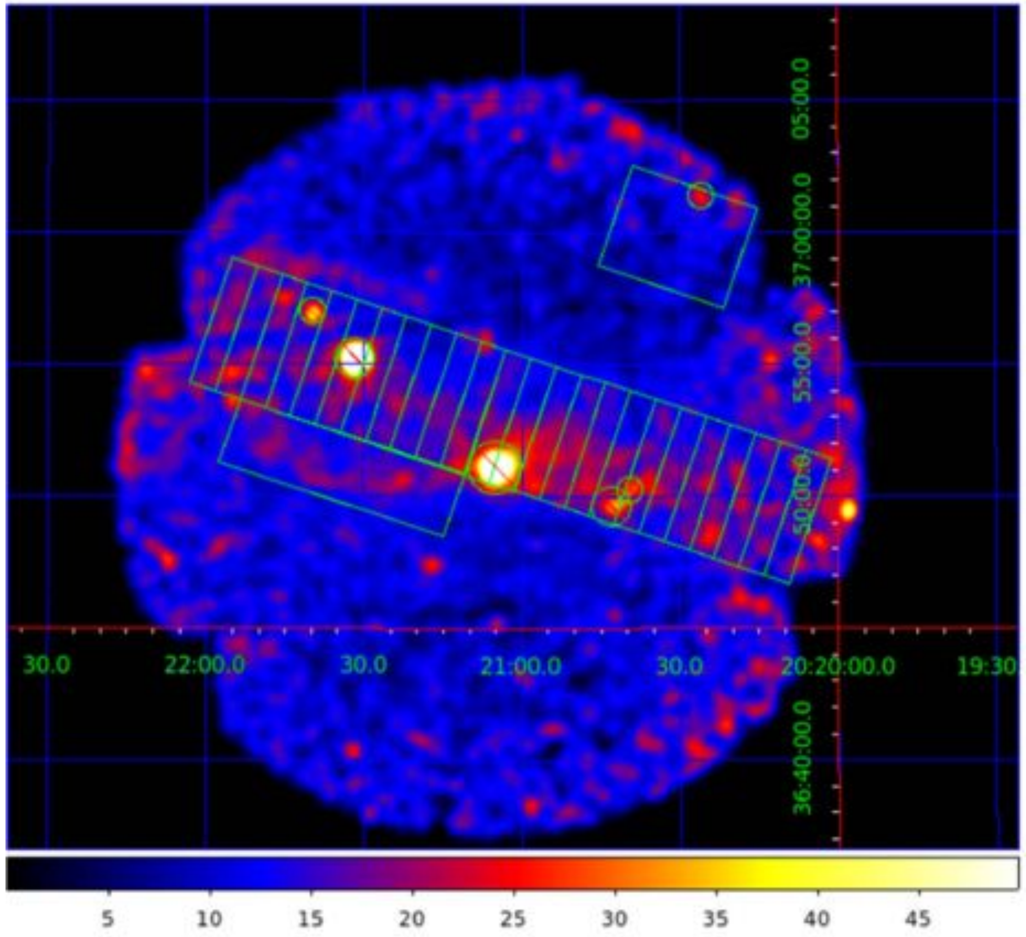

Da aggiornare :
- VERITAS : e' lo spettro vecchio (2014) sovrastimato
- u.l. fermi
- radio VLA ?

VER 2018+367

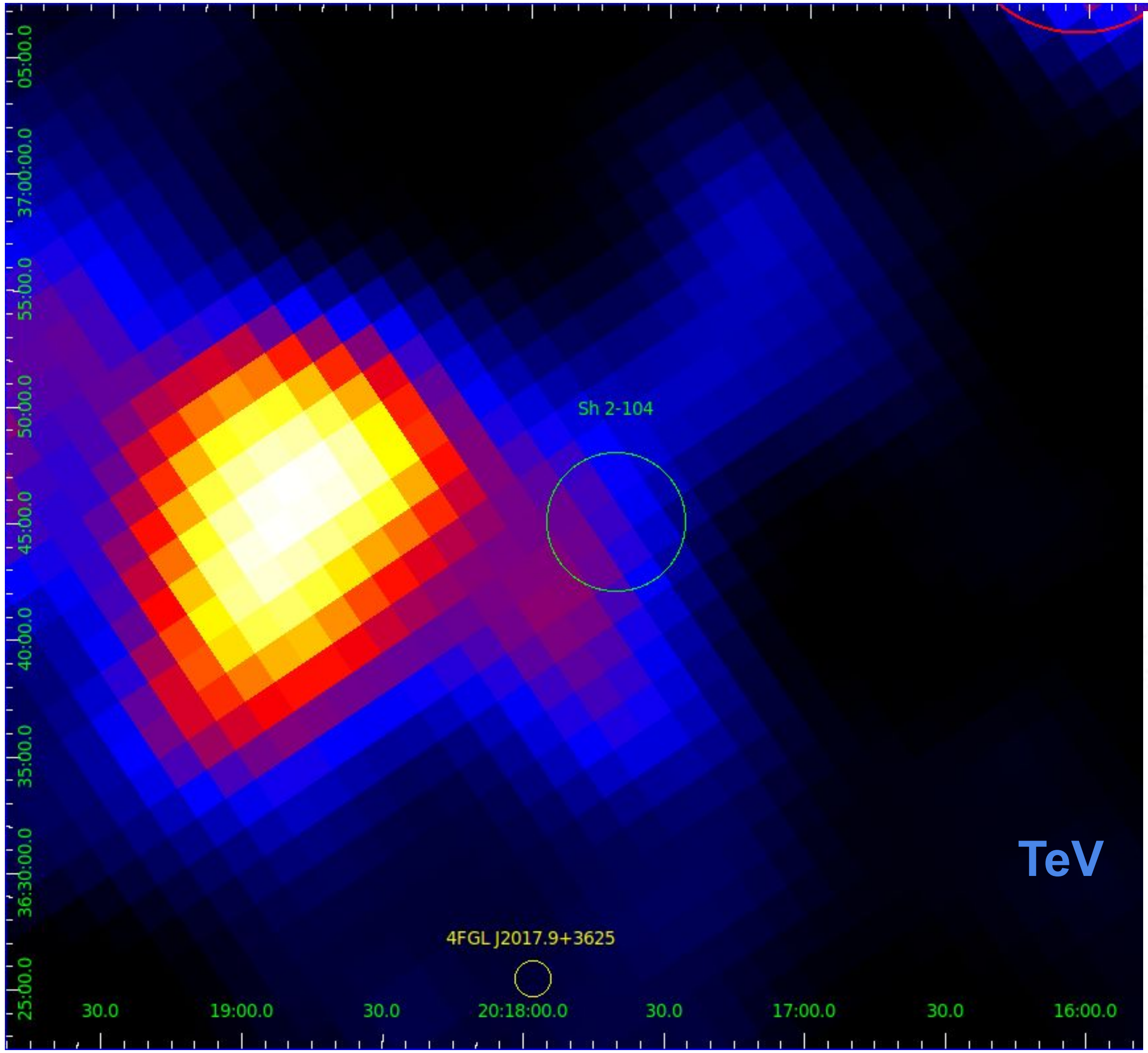

Sh 2-104
4FGL J2017.9+3625
TeV
30.0
19:00.0
30.0
20:18:00.0
30.0
17:00.0
30.0
16:00.0
05:00.0
37:00:00.0
55:00.0
50:00.0
45:00.0
40:00.0
35:00.0
36:30:00.0
25:00.0

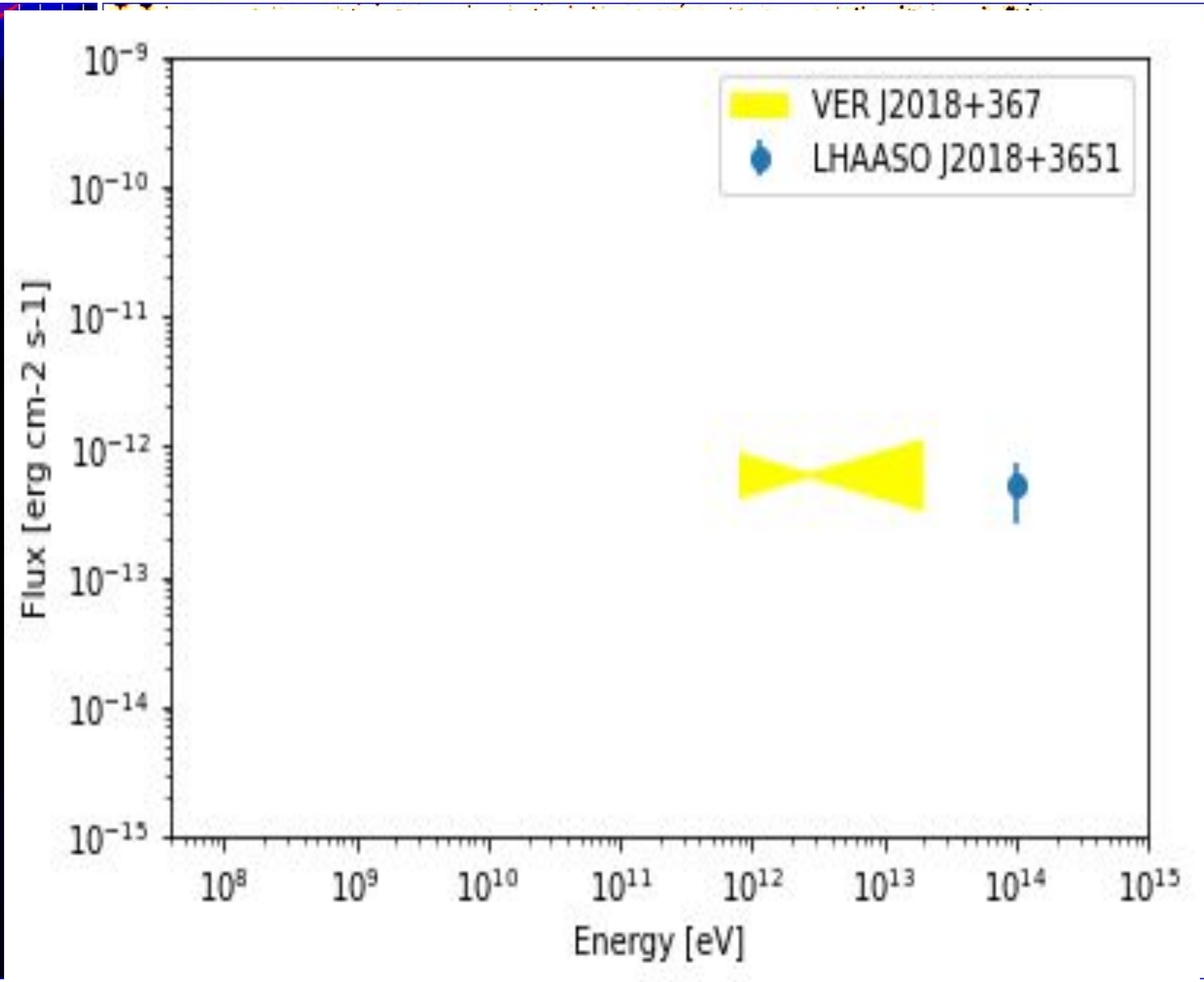

VER J2018+367
LHAASO J2018+3651
Flux [erg cm-2 s-1]
Energy [eV]
10^{-9}
10^{-10}
10^{-11}
10^{-12}
10^{-13}
10^{-14}
10^{-15}
10^{8}
10^{9}
10^{10}
10^{11}
10^{12}
10^{13}
10^{14}
10^{15}

VER 2018+367

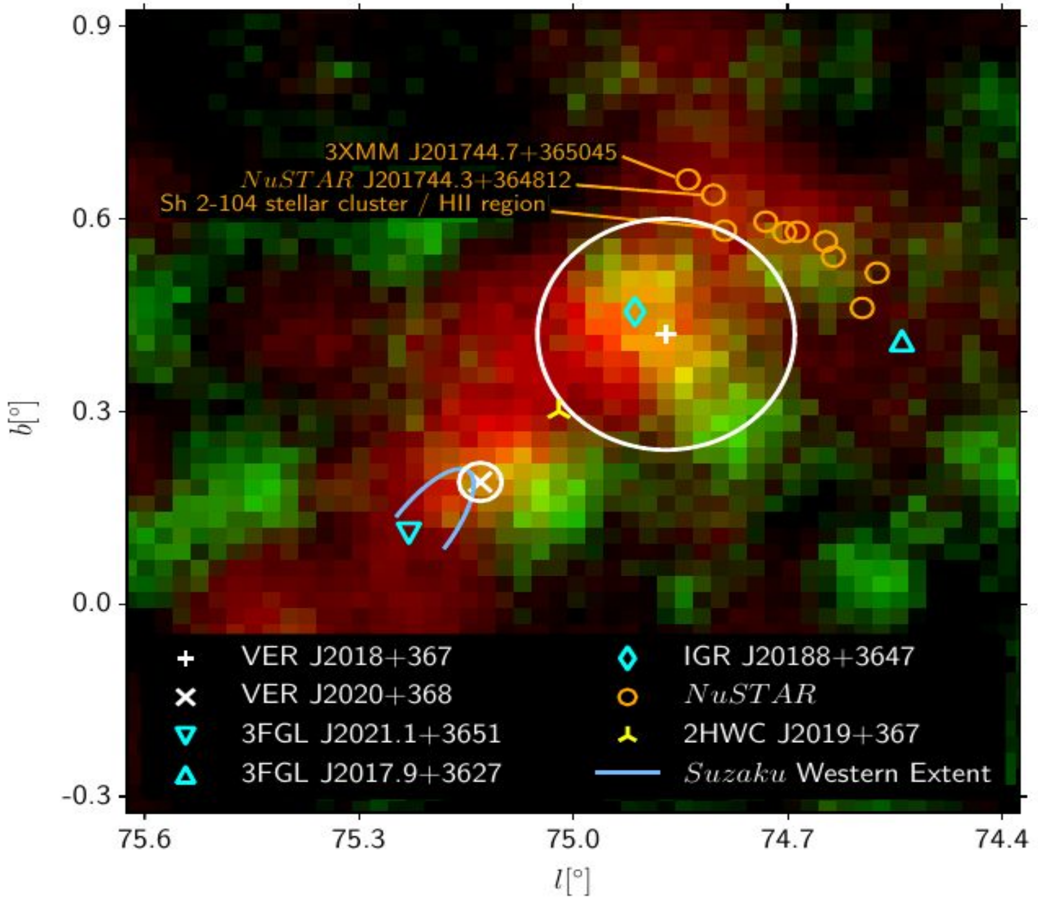

Figure 14. Energy dependent excess map at >1000 GeV (red) and <1000 GeV (green) for the region around VER J2019+368 produced using the *Point* integration region, the transition from black to color is an excess ≥ 0 with a maximum excess >1000 GeV of 70 counts and a maximum excess <1000 GeV of 30 counts. Unlike Aliu et al. (2014b) there is no evidence of a region of lower energy emission to the south of the extended emission from VER J2019+368. This is either due to the higher energy threshold employed in this analysis reducing the sensitivity to low energy emission in this region or the earlier result was a statistical fluctuation which has diminished with the increased data. VER J2018+367* and VER J2020+368* are shown with the 1σ extents (solid white lines) and are located at regions which show enhanced emission below 1000 GeV. Also shown are the locations of 2HWC J2019+367 (yellow, with the 1σ error on its position), IGR J20188+3647 (cyan diamond), the two *Fermi*-LAT pulsars (3FGL J2021.1+3651 and 3FGL J2017.9+3627 (cyan triangles)), and the *NuSTAR* sources from Gotthelf et al. (2016). The sky blue arc approximately traces the region with > 50 photons s^{-1} cm^{-2} sr^{-1} in the 2-10 keV energy range from Mizuno et al. (2017).